SPACE RESEARCH COORDINATION CENTER

EXCITATION AND RADIATIVE TRANSPORT OF OI 1304A° RESONANCE RADIATION

I. THE DAYGLOW

BY

D. J. STRICKLAND AND

T. M. DONAHUE

DEPARTMENT OF PHYSICS

SRCC REPORT NO. 101

UNIVERSITY OF PITTSBURGH
PITTSBURGH, PENNSYLVANIA

4 SEPTEMBER 1969

The Space Research Coordination Center, established in May, 1963, has the following functions: (1) it administers predoctoral and postdoctoral fellowships in space-related science and engineering programs; (2) it makes available, on application and after review, allocations to assist new faculty members in the Division of the Natural Sciences and the School of Engineering to initiate research programs or to permit established faculty members to do preliminary work on research ideas of a novel character; (3) in the Division of the Natural Sciences it makes an annual allocation of funds to the interdisciplinary Laboratory for Atmospheric and Space Sciences; (4) in the School of Engineering it makes a similar allocation of funds to the Department of Metallurgical and Materials Engineering and to the program in Engineering Systems Management of the Department of Industrial Engineering; and (5) in concert with the University's Knowledge Availability Systems Center, it seeks to assist in the orderly transfer of new space-generated knowledge in industrial application. The Center also issues periodic reports of space-oriented research and a comprehensive annual report.

NAS9-179

The Center is supported by an Institutional ~~Grant (NsG-416)~~ from the National Aeronautics and Space Administration, strongly supplemented by grants from the A. W. Mellon Educational and Charitable Trust, the Maurice Falk Medical Fund, the Richard King Mellon Foundation and the Sarah Mellon Scaife Foundation. Much of the work described in SRCC reports is financed by other grants, made to individual faculty members.

Excitation and Radiative Transport of OI 1304Å Resonance Radiation

I. The Dayglow

(Planetary and Space Science)

D. J. Strickland* and T. M. Donahue

Dept. of Physics, University of Pittsburgh

Pittsburgh, Pa.

August 1969

*Present address: Dept. of Physics, University of Florida, Gainesville, Fla.

Excitation and Radiative Transport of OI 1304Å Resonance Radiation†

I. The Dayglow

D. J. Strickland* and T. M. Donahue

The University of Pittsburgh

Pittsburgh, Pa. 15213 U. S. A.

Abstract

Radiative transfer theory is developed for the 1304Å triplet of atomic oxygen which includes the effects of pure absorption by molecular oxygen and variability of the temperature governing the relative populations of the ground state ^3P_j levels. Starting from an essentially complete intensity-height profile for the dayglow, the theory is used to determine the initial source function or the production rate. From the solution, we are able to discuss quantitatively the important dayglow excitation sources. The solutions are shown to be somewhat sensitive to the following parameters: (1) the oscillator strength f, (2) the temperature governing the Doppler line width, (3) the temperature governing the ^3P_j levels and (4) O_2 absorption below about 130 km. The assumption of complete frequency redistribution is applied and the basis of its validity is analysed with regard to the given problem.

A source is required in the F1 region whose strength is about 200 excitations per cm^3 per sec at 170 km. The altitude profile for the required source agrees well with those calculated for excitation of oxygen by supra-thermal photoelectrons.

†This work is based on a portion of the thesis submitted by D. J. Strickland to satisfy requirements for the Ph.D. in Physics at the University of Pittsburgh.

*Present address: Department of Physics, University of Florida, Gainesville, Florida.

1.0 INTRODUCTION

This is the first of two papers which will discuss transport of the resonance radiation of atomic oxygen in the Earth's upper atmosphere. In the present paper we treat the dayglow and in the second we shall consider the aurora. The radiation to be studied is a triplet at wavelengths of 1302-04-06Å, abbreviated hereafter as 1304Å. To date, a number of successful dayglow experiments have been performed in which altitude profiles of 1304Å radiation from about 100 km to 600 km have been recorded on sounding rockets (Fastie et al., 1964a; Fastie and Crosswhite, 1964b; Kaplan et al., 1964; Fastie, 1968; Heath, 1968). Several analyses of the early dayglow observations have been published (Donahue and Fastie, 1964; Tohmatsu, 1964; Donahue, 1965; Tohmatsu, 1965) indicating that the observed height profiles and apparent emission rates require the presence of a source in the thermosphere more important for excitation of the triplet than absorption of the solar emission lines. These analyses, however, were based on observations carried only to Aerobee altitudes, i.e., about 200 km. Such data do not extend high enough to show the form of the variation with height above the altitude of maximum brightness. This limitation, coupled with uncertainties about the absolute brightness of the airglow lines and about the absolute flux and spectral profile of the solar lines, has left a certain ambiguity in the assessment of the relative importance of the internal and external sources of excitation (Donahue, 1965). At the time these analyses were made, some high altitude data were available (Kaplan et al., 1964) but are difficult to explain in terms of reasonable models and are suspected of background contamination.

Recently, Fastie(1968) has observed the altitude profile of this dayglow feature from about 220 km to about 600 km during the flight of a

Javelin sounding rocket from Wallops Island in November 1964. The profile obtained at that time can be extended downward by normalizing it to the earlier Aerobee observations between 100 km and 220 km. Thus completed, it gives a sufficiently complete representation of the "typical" spatial profile of the airglow radiation field to reveal the distribution of the sources required to create it. This paper will show how a radiative transport calculation can determine these sources from the airglow information as well as how it can put some interesting limits on the range of atomic oxygen model atmospheres compatible with the observed radiation profile. The results require the presence of a strong internal source centered near 170 km to excite the $3s\,^3S_1$ level of atomic oxygen at a rate of about 200 cm^{-3} sec^{-1}. Regarding the density models, the variation of the resonance line brightness with altitude above 400 km where sunlight should be the principal source of excitation appears to demand more atomic oxygen in the atmosphere than the models appropriate for the time of the Javelin flight would call for. These points will be discussed in considerably greater detail after we have developed the transport theory for the 1304 triplet.

2.0 Atomic Properties and Temperature Dependence

The 1304 triplet arises from the transition $(2p)^4\,{}^3P_{2,1,0} - (2p)^3(3s)^1\,{}^3S_1$ which is designated as a resonance transition both because it is allowed and because the ground state (^3P) is involved. Such transitions are characterized by large oscillator strengths (f values) and in turn by large cross sections. The f value we originally chose for this work has the magnitude .021 (Parks et al., 1967). With such a small oscillator strength it proved impossible to reconcile the experimental altitude profile with reasonable oxygen abundances. A much larger f value seems to be needed. Recent measurements by Lawrence (1969) yield a value of 0.46 and F. Kaufman

(personal communication) reports that the value reported by Parks et al. (1967) is too low by a factor of about two. Theoretical f numbers have been calculated by Garstang (1961) (f - .051) and Kelly (1964) (f = .025). Using Lawrence's (1969) value of .046, we have recalculated our solutions and favor these in giving a physical interpretation for our results. As a point of interest, we present solutions in Section 6 for both f values showing the effects of changing this parameter.

The f value is related to the line center cross section σ_o for absorption of resonance radiation by the relationship

$$\sigma_o = \frac{\pi e^2}{mc} \frac{f}{\Delta\nu_D \sqrt{\pi}} \tag{1}$$

where the line has a Doppler profile and $\Delta\nu_D$ is the Doppler width given by

$$\Delta\nu_D = \lambda_o^{-1} \sqrt{\frac{2kT}{m(0)}} \tag{2}$$

We see by Equation (2) that σ_o is a function of the kinetic temperature T. This temperature varies from about 200° to as high as perhaps 1000° over the altitude range of interest in this study. Selected values of σ_o as a function of kinetic temperature for f = .021 and .046 are shown in Table 1. The values shown have been used to obtain the results which will be presented in Section 6.

The frequency dependent cross section $\sigma(x)$ is given by

$$\sigma(x) = \sigma_o \phi(x)$$

where $\phi(x)$ is the line profile and x is a measure of frequency in units of Doppler widths from the line center

$$x = (\nu - \nu_o)/\Delta\nu_D$$

In past work (Donahue and Fastie, 1964; Tohmatsu, 1964; Donahue, 1965; Tohmatsu, 1965) a pure Doppler line shape has been assumed. In this case

$$\phi(x) = e^{-x^2} \tag{3}$$

It is a well known fact that the contributions from the natural wings of the line become important in case considerable multiple scattering or imprisonment of the photons occurs. Such is the case for us in the lower regions of the atmosphere. Consequently, we have generalized $\phi(x)$ to the form

$$\phi(a, x) = \frac{a}{\pi} \int_{-\infty}^{\infty} \frac{e^{-\mu^2}}{a^2 + (x - \mu)^2}\, d\mu \tag{4}$$

In this form of $\phi(x)$ (the un-normalized Voigt function) $\underline{a}$ is a parameter specifying the strength of the wings of the line,

$$a = \frac{\gamma}{4\pi\ \Delta\nu_D}$$

γ being the transition probability or inverse lifetime of the excited state. The parameter $\underline{a}$, here referred to as the natural damping coefficient, may also be related to f by the relationship

$$a = \frac{2}{\lambda_o^2} \frac{g_1}{g_2} \frac{\pi e^2}{mc} \frac{f}{\Delta\nu_D} \tag{5}$$

(see Mitchell and Zemansky, 1961; Equations 33 - 39) where g_1 and g_2 are the statistical weights of the lower and upper states ($g_1/g_2 = 3$ for the

oxygen triplet). In addition to the cross section σ_o, selected values of $\underline{a}$ as a function of temperature for f = .021 and .046 are given in Table 1.

It can be seen that $\phi(a,x)$ depends on the kinetic temperature through both x and $\underline{a}$. In a situation in which $\Delta\nu_D$ varies by more than a factor of two, as it does for the temperature range we encounter, it would be desirable to include the variation in the transport problem. To do so, however, would make the calculations considerably more difficult and costly to perform. As is generally done in a problem of this nature, we have used constant values throughout the medium but have varied T as a parameter in such a way as to span the expected temperature range. From the results we can estimate how much effect the isothermal approximation has on our solutions.

The relative populations of atoms in the three levels of the ^3P ground term are assumed to be given by

$$p_j = g_j e^{-\Delta E_j/kT} \Big/ \sum_k g_k e^{-\Delta E_k/kT} \qquad (6)$$

where j = 2,1,0 and where the statistical weights g_j are 5,3 and 1 for the respective levels $^3P_2$, $^3P_1$ and $^3P_0$. We see that p_j is a function of temperature as are σ_o and $\phi(a,x)$. Table 2 gives p_j for various temperatures including the limiting values p_j = 5/9, 3/9 and 1/9 as $T \to \infty$. It should be pointed out that this temperature (hereafter referred to as the Boltzmann temperature T_B) does not necessarily equal the kinetic temperature governing the Doppler width, i.e., T_D. If the relative populations in the fine structure levels are influenced by collisions between atomic oxygen and ambient electrons (as suggested by Dalgarno and Degges, 1968), then T_B will differ from T_D and in fact will be greater than T_D. Transport processes involving both the 1304 triplet and the far infrared radiations resulting from the transition between the $^3P_{2,1,0}$ levels can also influence the

relative populations. Their effect would be to increase the populations of the $^3P_1$ and $^3P_0$ levels and the distribution would then not be describable strictly in terms of a temperature. Because of collisions between atomic oxygen atoms and surrounding particles throughout most of the medium, we shall assume that transport processes have a negligible effect on the relative populations and that the populations can be represented by T_B which may, however, be greater than T_D. It is a much simplier task to treat the case in which T_B varies through the medium than the case in which T_D varies. Accordingly, we have considered the effect of a variable T_B in our calculations. Usually T_B has been permitted to assume the ambient temperature but we have also considered an isothermal case with $T_B = 1000°$, chosen to represent a situation in which there is appreciable cooling of electrons by atomic oxygen.

With p_j a function of temperature, the optical depth for the j^{th} line at altitude z is given by

$$\tau_j = \sigma_o \int_z^\infty p_j(z')\, n(z')\, dz' \qquad (7)$$

As a function of frequency,

$$\tau_j(x) = \tau_j\, \phi(a,x)$$

When the medium is isothermal, the depth for one line can be related to that of another by

$$\tau_k = \frac{p_k}{p_j}\, \tau_j.$$

Such a relationship permits the transfer equations to be reduced to forms having explicit dependence on just one of the three depths and effectively reduces the treatment of the transport to a two level problem (Donahue, 1965). For the non-isothermal problem, a different variation of p_j for each j forces us to deal explicitly with each of the three depths in the transfer equations. Computationally, however, this introduces no difficulties provided we accurately relate one depth to another at each point in the medium.

Because molecular oxygen begins to absorb the 1304Å triplet below 120 km in a significant fashion, this absorption process has been incorporated into the transfer equations. In fact solution of these equations including true absorption has been obtained only for the case of auroral excitation where it is of particular interest (Donahue and Strickland, 1969). From those results, however, we can accurately estimate the effect on the dayglow (Section 7). The non-resonant cross section for O_2 is nearly independent of frequency in the neighborhood of the 1304Å triplet and is taken to be 5×10^{-19} cm^2 (Lee, 1955). We designate the corresponding optical depth by

$$t(z) = 5 \times 10^{-19} \int_z^\infty n(O_2)dz'$$

3.0 Transfer Equations

3.1 General Approach

The problem we set ourselves to is to determine the rate $S_o(\underset{\sim}{r})$ at which atomic oxygen must be excited into the $^3S_1$ level in order to produce the observed photon flux. The most likely contributions to S_o are from electron impact excitation, cascading from higher states, and absorption

of resonance radiation of solar origin. Obtaining the solution is complicated by the fact that the oxygen medium is optically very thick. This means that a photon emitted by an atom excited by one of the primary excitation events will be absorbed and thus excite another atom before it has travelled very far from its original source. The same in turn will be true of the resonance photon subsequently emitted by this atom. The result of this multiple scattering or imprisonment of resonance radiation is that the steady state density of excited atoms is much larger than the value it would have if each photon emitted were to escape the oxygen medium without recapture. The unidirectional flux of photons at a given point in the medium is determined by this steady state excitation rate or source function $S(\underset{\sim}{r})$. The rate of primary excitation $S_o(\underset{\sim}{r})$ represents only a very minor part of $S(\underset{\sim}{r})$, most of which is produced predominantly by capture of imprisoned photons.

The "apparent" column emission rate in photons/cm^2-sec-4π ster observed at $\underset{\sim}{r}$ in a direction $\cos^{-1}\mu$ from the vertical will be given by

$$4\pi I(\underset{\sim}{r},\mu) = \int S(\underset{\sim}{r}')\, T(\underset{\sim}{r} - \underset{\sim}{r}')\, dz'/\mu \qquad (8)$$

where $T(\underset{\sim}{r} - \underset{\sim}{r}')$ is a transmission function which depends on the number of atoms between $\underset{\sim}{r}$ and $\underset{\sim}{r}'$ in the direction of observation. If we are given $4\pi I$, the first step in determining the primary excitation rate is to invert Equation (8) and determine the final source function $S(\underset{\sim}{r})$. Unfortunately the process can be carried out only if a model for the atomic distribution is first adopted in order to specify $T(\underset{\sim}{r} - \underset{\sim}{r}')$.

With $S(\underset{\sim}{r})$ and the model atmosphere specified, the initial source function $S_o(\underset{\sim}{r})$ can then be found since $S(\underset{\sim}{r})$ must satisfy an integral equation of the type

$$S(\underset{\sim}{r}) = S_o(\underset{\sim}{r}) + \int S(\underset{\sim}{r}')G(\underset{\sim}{r} - \underset{\sim}{r}')d\underset{\sim}{r}' \qquad (9)$$

where G is an appropriate kernel relating the emission rate $S(\underset{\sim}{r}')$ at $\underset{\sim}{r}'$ to the excitation rate at $\underset{\sim}{r}$. The integral goes over the entire medium. To solve Equation (9) is not a trivial exercise, because S_o is usually very small compared to S and because the kernel is singular for vanishing values of its argument. As previously discussed, other complications also arise in practice because of the presence of pure absorption of the photons, notably by O_2, because variations in temperature cause variations in the width of the resonance absorption line profile and in the population of the fine structure levels of the ground state of atomic oxygen and finally because complex changes in the frequency of the photon occur upon scattering. All of these effects will be considered (not always rigorously) in the present treatment.

3.2 Complete Frequency Redistribution

In the initial formulation of the transport problem, a two level atom will be assumed. Accomodation of the fine structure splitting of the ground state of atomic oxygen will be made in the next section. It will further be assumed that the geometry of the medium is plane parallel with the density of absorbers functions of z only. This is a very good approximation in the present application where the sun is reasonably high in the sky and the scale height of oxygen is of the order of one percent of the radius of the Earth.

In this section we shall investigate the criteria which determine the applicability of complete frequency redistribution (CFR) to a transport problem. By definition CFR requires that the frequency profiles for both initial excitation and scattering from a unit volume have the same

frequency dependence as the absorption profile. In any state of equilibrium in which the collision rate between excited atoms and surrounding particles exceeds the transition probability for the given state, the above condition is at least approximately satisfied; in particular, both the emission and absorption profiles are represented by the Voigt function. When the collision rate is significantly less than the transition probability, a unique relationship exists between the frequency and direction of an incoming photon and those of the outgoing photon for a given absorber of velocity $\underset{\sim}{v}$. In such a case it is not nearly as simple to establish that CFR is applicable. We shall now consider in a semi-quantitative way, how accurately the emission profiles can be represented by Voigt functions.

For a plane parallel geometry, the basic equation of radiative transfer is

$$\mu \frac{dI}{dz} = - k(x,z)\ I(x,\mu,z) + \varepsilon(x,\mu,z) \tag{10}$$

where I is the frequency dependent intensity given in photons/cm^2-sec-ster-$\Delta\nu_D$ in the direction $\mu = \cos\theta$, $k(x,z)$ is the absorption coefficient and $\varepsilon(x,\mu,z)$ is the emissivity or number of photons emitted/cm^3-sec-ster-$\Delta\nu_D$. The absorption coefficient $k(x,z)$ when expressed explicitly in terms of its frequency is $k_o(z)\phi(a,x)$, $\phi(a,x)$ being the Voigt profile in this work. Expressed in terms of the optical depth τ_x, Equation (10) becomes

$$\mu \frac{dI}{d\tau_x} = - I(x,\mu,\tau) + S(x,\mu,\tau) \tag{11}$$

where $d\tau_x = k_o\phi(a,x)dz$ and $S(x,\mu,\tau)$, the total source function, is the ratio of ε to $k(x,z)$. The intensity I is the same function whether we index it by τ or z. For CFR, we note that S is not a function of x because ε possesses

the same frequency dependence as does k. The formal solution to Equation (11) is

$$I(x,\mu,z) = I_o(x,\mu)e^{-\tau\phi(a,x)} + \int S(x,\mu,\tau')e^{-|\tau-\tau'|\phi(a,x)/\mu} d[\tau'\phi(a,x)]/\mu \quad (12)$$

The first term on the right contains the contribution from the attenuated flux of radiation incident on the medium from outside. The second term represents the flux resulting from emission with the medium along direction μ. A complication in using this solution arises from the fact that ϵ is a function of I_x not only at frequency x but at all other frequencies as well. For the condition of radiative equilibrium, we may write ϵ as

$$\epsilon(x,\Omega,z) = \epsilon_o(x,\Omega,z) + \int I(x',\Omega',z)R(x,x',\Omega,\Omega',z)\, dx'd\Omega' \quad (13)$$

This relationship expresses the condition that the emissivity must equal the rate at which photons of frequency x are created in a unit volume plus a scattered contribution from that volume. The quantity R, referred to as the redistribution function describes this scattering and is the probability for a unit volume that an incoming photon of frequency x' and direction Ω' is absorbed and re-emitted at frequency x in direction Ω. For the situation in which collisions are unimportant, re-emission is isotropic, and the wings of the spectral lines are included, R has the form

$$R = \frac{k_o(z)}{4\pi\sqrt{\pi}} \frac{1}{\sin\theta} \exp - \left[\frac{(x - x')}{2} \csc\frac{\theta}{2}\right]^2 \phi\left(a \sec\frac{\theta}{2}, \frac{(x + x')}{2} \sec\frac{\theta}{2}\right) \quad (14)$$

where θ is the angle of scattering. This form of R was originally introduced by Henyey (1940) and more recently analyzed by Hummer (1962). A property of R which will be useful below is described by the following requirement of reversibility

$$\int R\, dx' = \frac{k_o}{4\pi}\, \phi(a,x) \tag{15}$$

If we wish, we can now immediately integrate Equation (15) over direction and obtain

$$\int R\, dx'\, d\Omega' = k_o \phi(a,x) \tag{16}$$

Because of the symmetry, we can also, if we wish, consider x' and Ω' as either the incoming or the outgoing variables. If they are interpreted as outgoing variables, we must, in fact, obtain $k_o\phi$ in Equation (16) since from the above definition of R, an integration over all outgoing directions and frequencies must leave us with the probability (per unit length) of absorption at frequency x .

For the case in which collisions are important, the redistribution function, defined similarily to R above and here designated by R_c has the simple form

$$R_c(x,x') = \frac{k_o}{4\pi\sqrt{\pi}}\, \phi(a,x)\ \phi(a,x')$$

We immediately see that R_c satisfies the same relationships as those expressed in Equations (15) and (16) for R and has the same symmetry properties.

Let us now consider Equation (13), i.e. radiative equilibrium, when the intensity is independent of frequency although not necessarily isotropic. Equations (15) and (16) show that the scattering contribution to ε is just $J(z)\, k_o\, \phi\,(a,x)$ where $J(z)$ is the effective flux entering the unit volume in photons/cm^2 - sec - $\Delta\nu_D$. Because R_c satisfies Equations (15) and (16), this result holds for R_c as well as R even though each redistribution function describes entirely different scattering processes. A close study of the properties of the redistribution function R shows that when x' is small the frequency x of the re-emitted photon has a large probability of being anywhere in the frequency range where the Voigt profile is almost Doppler in shape - in the so called core of the line. When x' lies in the range of frequencies so large that the Voigt profile almost has the natural line shape the scattering is almost coherent and x is very nearly the same as x'. Physically this behavior reflects a contest for photons between the natural line absorption profile and the Maxwell-Boltzmann distribution. For frequencies close enough to the line center the preference is for capture at the center of the natural line by sufficiently fast atoms while for frequencies far from the center capture in the natural wings by slow atoms predominates over capture by atoms in the tail of the Maxwell distribution. Thus, if one actually applies R to a transport problem, frequency redistribution occurs at small frequencies but gives way to coherency in the wings. If we now consider R_c, we see that a photon absorbed at x' = 0 has a distinct probability - varying with the line profile $\phi(x)$ - of being re-emitted in the wings, even the far wings. On the other hand, a photon captured far in the natural wings has its greatest probability of re-emission at x = 0. In the problem we treat in this paper the redistribution of frequencies is really described by $R(x,x',r,r',z)$. It is our hope, however, that throughout most of the medium, the intensity varies weakly enough over the important

frequency range that scattered radiation is roughly described by a Voigt profile, thus allowing us to replace R by the much simpler function R_c. We emphasize, however, that R_c is not the proper redistribution function physically, in our case.

With complete frequency redistribution, the scattered radiation from a unit volume possesses a Voigt profile. From Equation (13), it then follows that the total emission rate ε also possesses this profile provided the initial rate ε_o does. To apply CFR validly

1) ε_o must approximately possess a Voigt profile

2) $I(x,r,z)$ must be approximately independent of frequency.

Regarding condition (2), it will usually be sufficient if the frequency independence extends out to about $x \simeq 3$. Were $I(x,r,z)$ independent of frequency over an unlimited range, we would find that most of the absorption occurs over the region $|x| \lesssim 3$ for the values of the damping coefficient appropriate to this study.

In the case to be treated in this paper the initial source function should possess a profile closely resembling a Voigt profile because of the nature of its excitation. The dominant source of excitation is probably electron impact on atomic oxygen and thus will produce an initial source with roughly the required profile. To investigate the second criterion, we have calculated the intensities of the 1302, 04, 06Å lines at various depths in the medium as a function of both frequency and direction. Figure (1) shows examples of these at a depth $\tau_2 = 600$ for one of our earlier models with $f = .02$. The source functions from which these profiles were derived were themselves obtained in the CFR approximation. If the intensity implied by these source functions were to violate the second criterion seriously that in itself would have shown a gross inconsistency in the application of the approximation. We believe, however, that these results

present a realistic picture of the true intensities. This is based in part on several more critical and detailed analyses of the condition of CFR (see e.g. Holstein, 1947, Hearn, 1964, and Doschek, 1969). Holstein (1947), for example, was the first to show that interior to the medium, CFR will generally be valid in the core of the line.

Considering Figure (1), we see that the intensity profile is generally flat to about x = 2. The reason the 1306Å profiles are the narrowest is that the total effective optical depth τ_o is smallest for the 1306Å line. Although the frequency independent portion of none of these profiles extends to values of x as large as we would like, say to $|x| \gtrsim 3$, still an appreciable fraction of the absorption which would result from a perfectly flat profile does come for values of x between +2 and -2. For the intensity profiles shown, the resulting emissivities for scattered radiation would closely resemble the Voigt profile in the core (or the e^{-x^2} portion of the line) but would show a deficiency in the wings. And, indeed, in the real case described by the exact redistribution function, the emissivity is deficient in the wings, because of the tendency of photons in the wings to escape the medium after a few scatterings.

The deficiency of wing photons illustrated in Figure (1) shows, however, that the CFR approximation unrealistically enhances the emissivity in the wings of the line. If we now consider Figure (2) which shows intensities evaluated very close to the upper boundary, we see that CFR tends to break down there. It is not very far from the boundary, however, that the situation regarding the intensity profiles improves considerably. So, over most regions of the medium, as long as the examples in Figure (1) are typical of the true intensities, CFR should not yield results significantly different than those obtained in an exact calculation. The investigations referred to above all indicate that this is indeed the case.

Now assuming CFR, the total emission rate can be expressed as

$$\varepsilon(x,\Omega,\ z) = \varepsilon(z)\quad \phi(a,x)/4\pi\sqrt{\pi}$$

where $\phi/\sqrt{\pi}$ is the normalized Voigt profile and $1/4\pi$ normalizes ε for isotropic emission. The source function, originally introduced as $S(x,\mu,\tau)$ becomes

$$S(x,\mu,\tau) = \frac{\varepsilon(z)}{k_o}\ \frac{1}{4\pi\sqrt{\pi}}$$

and is seen to be independent of x and μ. In the treatment to follow, we choose to define the total source function by

$$S(\tau) = \frac{\varepsilon(z)}{k_o}$$

which represents the total emission rate per cm^2 and per unit optical depth. The total emissivity is then

$$\varepsilon(x,z) = k_o\ S(\tau)\ \frac{\phi(a,x)}{4\pi\sqrt{\pi}} \tag{17}$$

Similarily

$$\varepsilon_o(x,z) = k_o\ S_o(\tau)\ \frac{\phi(a,x)}{4\pi\sqrt{\pi}} \tag{18}$$

Replacing R by R_c in Equation (13) and dividing out the common factor $k_o\phi/4\pi\sqrt{\pi}$ we now obtain

$$S(\tau) = S_o(\tau) + \int I(x',\mu',\tau)\phi(a,x')dx'\ 2\pi d\mu' \tag{19}$$

Equation (12) allows us to express this as

$$S(\tau) = S_o(\tau) + \int S(\tau') \frac{\phi^2(a,x)}{2\sqrt{\pi}} e^{-|\tau - \tau'|\phi(a,x)/\mu'} dx' \frac{d\mu'}{\mu'} d\tau' \qquad (20)$$

Here, the contribution of the attenuated external radiation source has been lumped in the S_o term along with internal excitation sources. It should be pointed out that if one wishes to solve this equation by initially specifying S_o for an external radiation source, special considerations must be given as to how S_o is evaluated. Deep in the medium if S_o were to represent the actual rate of initial excitation produced by the external radiation source we would find it heavily dominated by wing photons due to the ever increasing reversal of the attenuated external flux as it penetrates the medium. Most of the photons resulting from this excitation are far enough in the wings that they would escape the medium almost immediately. Hence, to choose an effective CFR S_o, we would have to judiciously discard most of actual wing dominated S_o, discarding an ever increasing fraction deeper into the medium (Donahue, 1965). Fortunately, we can ignore this difficulty since our objective is to derive S_o from the intensity.

If we now introduce the transport kernel

$$H(|\tau - \tau'|) = \frac{1}{2\sqrt{\pi}} \int \phi^2 e^{|\tau - \tau'|\phi/\mu'} \frac{d\mu'}{\mu'} dx' = \frac{1}{2\sqrt{\pi}} \int \phi^2 E_1(|\tau - \tau'|) dx' \qquad (21)$$

Equation (20) takes the form

$$S(\tau) = S_o(\tau) + \int S(\tau') H(|\tau - \tau'|) d\tau' \qquad (22)$$

H is the probability per unit optical depth at τ that a photon upon emission from the level τ' will reach the level τ and be absorbed.

The intensity resulting from emission within the medium can be expressed as

$$I(x,\mu,\tau) = \int S(\tau') \frac{\phi(a,x)}{4\pi\sqrt{\pi}} \; e^{-|\tau - \tau'|\phi/\mu} \phi(a,x) d\tau'/\mu \qquad (23)$$

Integration over x permits Equation (23) to be written in the form

$$4\pi I(\tau,\mu) = \int S(\tau')\, T(|\tau - \tau'|/\mu)\, d\tau'/\mu \qquad (24)$$

where

$$T(|\tau - \tau'|/\mu) = \frac{1}{\sqrt{\pi}} \int \phi \; e^{-|\tau - \tau'|\phi/\mu} \, dx \qquad (25)$$

The transmission function, $T(|\tau - \tau'|/\mu)$ is the probability that a photon will be emitted and will travel the distance $|\tau - \tau'|/\mu$ without an absorption. Equations (22) and (25) are the CFR forms of the transfer equations for a two level atom where the medium can be represented by a plane parallel geometry. In the following section we shall modify this formulation by incorporating in it absorption and the fine structure of the ground state of atomic oxygen.

3.3 Introduction of pure absorption and fine structure

Pure absorption has the effect of increasing the effective attenuation along a photon's path. We take account of this loss of photons by properly altering the probability functions T and H. The new transport functions, $T'(|\tau - \tau'|/\mu, |t - t'|/\mu)$ and $H'(|\tau - \tau'|, |t - t'|)$ become

$$T'(|\tau - \tau'|/\mu,\ |t - t'|/\mu) = \frac{1}{\sqrt{\pi}} \int \phi(a,x)\ e^{-[|\tau - \tau'|\phi(a,x) + |t - t'|]/\mu}\, dx$$

$$= e^{-|t - t'|/\mu}\ T(|\tau - \tau'|/\mu) \qquad (26)$$

and

$$H'(|\tau - \tau'|,\ |t - t'|) = \frac{1}{2\sqrt{\pi}} \int \phi^2(a,x)\ E_1(|\tau - \tau'|\phi(a,x) + |t - t'|)dx \qquad (27)$$

To take into account the fine structure of the ground state of oxygen we note that all emissions arise from the single level $^3S_1$. This allows us to designate S as the total source function despite the fact that the resulting emissions separate into three distinct lines. If, however, we desire that part of S which produces the 1302Å line, for example, we have

$$S_2 = \frac{5}{9} S$$

or more generally for the j^{th} line

$$S_j = g_j' S \qquad (28)$$

where g_j' is the ratio $g_j/\Sigma_k\ g_k$. The same considerations also apply to the initial source function S_o. In solving the transfer equations, S and S_o may be expressed as a function of any of the three depths. We choose to write them as functions of τ_2 and as such they are then given in units of photons/cm^2-sec-unit τ_2. If we wish to transform from one depth to another, we can use the transformation

$$S(\tau_k) = \frac{p_j}{p_k} S(\tau_j) \qquad (29)$$

and do similarily for S_o. The contribution of S to the j^{th} line (Equation 28) may then be written as a function of any chosen depth τ_k in the form

$$S_j(\tau_k) = g_j' \, S(\tau_k) \tag{30}$$

where k need not equal j and $S_j(\tau_k)$ is the rate at which the j^{th} line is emitted per unit τ_k.

Now, considering the first of the transfer equations, the intensity in the j^{th} line is

$$4\pi I_j(\tau_j,\mu) = \int S_j(\tau_j')T'(|\tau_j - \tau_j'|/\mu, \; |t - t'|/\mu)d\tau_j'/\mu \tag{31}$$

Experimentally, only the sum of the three lines was measured in a vertically upward direction and as such the observed intensity is expressed by

$$4\pi I(\tau_2) = \sum_j g_j \int S(\tau_j')T'(|\tau_j - \tau_j'|, \; |t - t'|)d\tau_j \tag{32}$$

where τ_2 on the left is used simply as an index of the level at which the intensity is evaluated.

The total source function $S(\tau_2)$ is comprised of $S_o(\tau_2)$ plus scattered contributions arising from excitation by each of the three lines. For the j^{th} line, this latter contribution is

$$g_j \int S(\tau_j')H'(|\tau_j - \tau_j'|, \; |t - t'|)d\tau_j$$

This term, however, is in the form of an excitation rate per unit depth τ_j in the appropriate line. To add the contributions of the three lines, they

must each be changed to rates per unit τ_2 and from Equation (29), this requires that each be multiplied by p_j/p_2. The transport equation then becomes

$$S(\tau_2) = S_o(\tau_2) + \sum_j \int g_j \frac{p_j}{p_2} \; S(\tau_j) H(|\tau_j - \tau_j'|, |t - t'|) d\tau_j' \qquad (33)$$

From the nature of our problem, considering the large optical depths involved plus the addition of pure absorption, difficulty was encountered in obtaining a smooth function for S_o. Because solving the above equation required much of our effort, a discussion of the sources of error and the final workable form for this equation as well as Equation (32) are given in the Appendix.

4.0 Data and Atmospheric Models

The height profile of the intensity is shown in Figure 3 and represents a composite from two experiments (Fastie, 1968). During these flights the solar zenith angle was 60°. For the time of the high altitude flight, the Jacchia (1965) model predicts an exospheric temperature of 850°. An atmospheric model appropriate to this temperature is given in Table 3 (A. I. Stewart, personal communication). As will be discussed shortly, a requirement regarding the behavior of the total source function $S(\tau)$ suggests the possibility that a higher exospheric temperature existed during the time of the high altitude flight. To account for this possibility, we have also considered a model having an exospheric temperature of 1000° (Table 4). that part of the model above 120 km was taken from U.S. Standard Atmosphere Supplements, 1966 and that below from Colegrove et al. (1966), the latter being scaled so as to join smoothly at 120 km. In Tables 3 and 4, the optical depths τ_2, τ_1 and τ_0 are included to show their range in the problem. The particular sets given refer to $T_D = 850°$ and $1000°$ respectively

and T_B equal to the appropriate ambient temperature profiles.

5.0 Total Source Function Near the Upper Boundary

In the course of solving the transfer problem, we have obtained solutions for both f = .021 and f = .046. The basic model used with f = .021 has a 1000° exospheric temperature (Table 4). Two models were used with f = .046, the 1000° model just mentioned and another with an 850° temperature (Table 3). Table 5 shows the particular models for the various solutions we have obtained.

Based on the Jacchia model, we originally solved the transfer problem using the 850° model and f = .021. Trouble immediately developed because of an upturning of $S(\tau_2)$ near $\tau_2 = 0$. A requirement inherent in the transport theory is that $S(\tau)$ monotonically decrease as the boundary is approached and, in fact, possess an infinite slope at $\tau = 0$. The condition at the boundary is readily demonstrated if we differentiate the transport equation. Initially we have

$$\frac{dS}{d\tau} = \frac{dS_o}{d\tau} + \int S(\tau') \frac{d}{d\tau} H(|\tau - \tau'|)d\tau' \tag{34}$$

From equation (21), $\frac{dH}{d\tau} = -\frac{dH}{d\tau'}$, and consequently, by replacing $\frac{dH}{d\tau}$ with $-\frac{dH}{d\tau'}$ and integrating by parts, we obtain

$$\frac{dS}{d\tau} = \frac{dS_o}{d\tau} + S(o)H(\tau) - S(\tau_o)H(\tau_o - \tau) + \int \frac{dS}{d\tau'}(\tau')H(|\tau - \tau'|)d\tau' \tag{35}$$

As $\tau \to 0$, $H(\tau) \to \infty$ which is sufficient to establish that $\frac{dS}{d\tau} \to \infty$. Away from the boundary $S(\tau)$will continue to increase to a peak located well into the medium. Even with an external source of excitation, $S(\tau)$ peaks well away

from the boundary because of imprisonment which is strongest at the center of the medium.

To correct the behavior of $S(\tau_2)$ requires greater optical depths near the 600 km level. For this reason, the 1000° model was applied to the problem and this resulted in a considerable improvement although a slight upturning still persisted. Another method of increasing the optical depth is to increase the f value. Therefore, we adopted Lawrence's (1969) value of .046 and recalculated $S(\tau_2)$ for both exospheric temperatures. The results are shown in Figure 4 along with two other solutions to be discussed shortly. The positive gradient in S still persists at 850° but is essentially or nearly corrected at 1000°.

If we are to believe that the 850° model is actually the more appropriate one, we must then consider sources of this pathological behavior in S other than a lack of optical depth. One such source might be the breakdown of CFR near the boundary. This can be ruled out as a problem however, since for small optical depths, the CFR solution $S(\tau)$ must, in fact, approach the true $S(\tau)$ and both in turn must approach the solution for the case of no attenuation. To represent this latter solution near the boundary, we divide the medium into zones and consider average values of S over each zone. For the first two zones,

$$\bar{S}_1 = 4\pi I_1/\Delta\tau_1$$

and

$$\bar{S}_2 = (4\pi I_2 - 4\pi I_1)/\Delta\tau_2$$

where $4\pi I_1$ and $4\pi I_2$ are the observed intensities at the bottom of zones 1

and 2 and $\Delta\tau_1$ and $\Delta\tau_2$ are the zone widths. The resulting solutions for the 850° and 1000° models are included in Figure (4) along with the CFR solutions. Because the actual emission profile corresponding to the true $S(\tau)$ shows a predominance of wing photons near the boundary, initially the true solution will not differ much from that with no attenuation but more specifically will lie between the solutions for this and the CFR case. Since all solutions exhibit an upturning in Figure (4), so must the exact solution and we thus conclude that the assumption of CFR is not responsible for the effect.

Another possibility is that $4\pi I$ actually decreased more rapidly with increasing height than the data indicated. This is difficult to believe, however, since the unresolved triplet was observed with a spectrophotometer, the resolution of which was sufficient to rule out spectral contamination. Unless there was a time dependent source of absorption not properly corrected for, the relative intensities recorded should be reliable. Although we have not satisfactorily resolved the question, the best explanation seems to be that larger optical depths are called for. If we assume the f value is no larger than .046, this requires us to abandon the 850° model in favor of one with a higher exospheric temperature, one in the vicinity of 1000°, or somehow to introduce considerably more oxygen at high altitudes.

6.0 Temperature Effects Exhibited by the Transfer Solutions

In Table 5, we have listed models in terms of the parameters f, T_D and T_B. The solutions we have obtained for them show sufficient differences that a brief analysis of the various effects is in order. Before proceeding to compare the various solutions, it is worth noting that a change in f has exactly the same effect as changing T_D. Provided T_D is taken to be constant throughout the medium, then T_D as well as f enter the transfer

equations only through σ_o and $\underline{a}$ (Equations (1) and (5)). The relationship is an inverse one such that increasing f has the same effect as decreasing T_D by an appropriate amount. In the following analysis, we first show the effects produced by changing T_B and then T_D. It will then be straightforward to compare solutions for differing f values since the effect is the same as changing T_D.

To show the effects of changing T_B and T_D, we consider solutions for f = .046 and T_{ex} = 850°. Changing the exospheric temperature from 850° to 1000° has a negligible effect on S_o at low altitude and so we shall confine this discussion to the 850° model. In Figure (5) are shown the total source functions $S_{3V(b)}(z)$ and $S_{3C(b)}(z)$. These are solutions for a kinetic temperature of 300°K but for a variable T_B and for a T_B constant at 1000° respectively. The subscript b denotes the models in which T_{ex} is 850° and f is 0.046. Because each of these solutions relates to the same intensity profile, it follows that model 3C is the more opaque model requiring a greater source function than 3V. If we consider individual optical depths, we see from Equation (7) that τ_1 and τ_0 of 3C increase relative to those of 3V as the altitude decreases while the reverse happens to τ_2. The fact that S_{3C} is greater than S_{3V} indicates that relative increases in τ_1 and τ_0 more than compensate for the relative decrease in τ_2. Thus the effective opacity of 3C is greater than 3V as measured by the transmission function relating S(z) to $4\pi I$.

The initial source functions $S_o(z)$ as obtained from S(z) by use of Equations (A4) are compared for models 3C and 3V in Figure (6). Generally the medium with the greater opacity will provide greater amplification of S_o by imprisonment, as the escape function, E, is smaller. Thus a smaller S_o is required to produce a given S(z) at a given altitude. This effect is not great enough, however, to reduce S_o^{3C} very much relative to S_o^{3V} despite the greater opacity of 3C in comparison with 3V.

The effect of changing Doppler temperatures can be seen in Figure (6) where S(z) are compared for models 3C(b) and 8C(b), in which the Doppler temperatures are 300° and 850° respectively but T_B is constant at 1000°K. The line center optical depths are larger for the 300° case than for the 850° case by a factor of 1.68. Thus where transport occurs mainly in the Doppler core of the lines model 8C is more transparent than model 3C and requires a smaller source function. This is the case above 160 km. At lower altitudes, however, the optical depths become so great that the wings dominate the transport. In this situation, the medium of 3C actually becomes more transparent than that of 8C thus requiring less source function as Figure (6) indicates. Quantitatively this effect can be understood if $\phi(x)$ is represented, as it can be, by

$$\phi(x) \tilde{=} e^{-x^2} \quad , \; x << x_c$$

$$\phi(x) \tilde{=} \frac{a}{\sqrt{\pi}} \frac{1}{x^2} \; x >> x_c$$

where

$$e^{-x_c^2} = \frac{a}{\sqrt{\pi}} \frac{1}{x_c^2} \tag{36}$$

Then

$$T(|\tau - \tau'|) = \frac{1}{\sqrt{\pi}} \int_{-\infty}^{+\infty} e^{-x^2} e^{-|\tau - \tau'|} e^{-x^2} dx \tag{37}$$

when $|\tau - \tau'|$ is small, and

$$T(|\tau - \tau'|) \simeq \frac{2a}{\pi} \int_{x_c}^{\infty} \frac{1}{x^2} e^{-|\tau - \tau'| \; a/\sqrt{\pi} \; x^2} dx \qquad (38)$$

when $|\tau - \tau'|$ is large. Between the 120 km and 140 km levels the optical distances in the 1304Å line are 7800 and 4637 for the 300° and 850° Doppler temperatures respectively. However, the transport functions, given practically by Equation (38) are 8.39×10^{-4} and 8.00×10^{-4} for 3C and 8C respectively.

The initial source functions $S_o(z)$ required to produce S_{3C} and S_{8C} are shown in Figure (8). S_o^{3C} dominates S_o^{8C} relatively more than S_{3C} dominates S_{8C} even at high altitude. This indicates that medium 3C is not particularly efficient compared to 8C in trapping photons despite the greater line center opacity. The reason is that large slant paths are involved in determining the escape probability E and the transport kernel H. Because of the effect of the wings the model 8C remains a more effective imprisoner of photons than 3C up to fairly high altitudes.

In Figures (9) and (10), in addition to the initial source functions just discussed for models 3C(b), 3V(b) and 8C(b), are shown the excitation rates required for models 8V(b), 3C(a), 3V(a), 10C(a) and 10V(a). The last four cases, shown in Figure (10), are the models in which the oscillator strenth assumed was 0.021 and the exospheric temperature was 1000°K. The similarity of the profiles for cases 8(b) and 3(a) is a consequence of the effect we have mentioned above, that increasing the oscillator strength is equivalent to reducing the Doppler temperature. The development of a bimodal structure in S_o as the Doppler width increases and the line center opacity diminishes is interesting in view of the possible importance of dissociative photon excitation as a source of $^3S_1$ atoms at low altitudes. We shall discuss this point at greater length in the next section.

7.0 Excitation Mechanisms

In Figure (11) the initial source functions or excitation rates for the $O(^3S_1)$ term required to account for the rocket intensities are shown for two models. These are 8C(b),(850° Exospheric temperature and Doppler temperature, constant 1000° Boltzmann temperature and an oscillator strength of 0.046) along with model 10C(c) which is the same as model 8C(b) except that T_∞ and T_D are 1000°. The second model therefore contains more atomic oxygen than the first at high altitudes and has a considerably greater line center opacity. In both models there are clearly two principal source regions. One source maximizes above 400 km and is about two orders of magnitude weaker than the other which has a maximum at about 170 km.

Presumably the high altitude source is provided by absorption of solar photons in the three solar OI resonance emission lines. The contribution to S_o from this source should be given by

$$S_o(z) = \sum_k (\pi F\nu)_k \sqrt{\pi}\, \Delta\nu_D\, T(\tau_k/\mu_o)\, \sigma_o\, p_k n(z)$$

where μ_o, the cosine of the solar zenith angle, is 0.5 in our case and $(\pi F\nu)_k$ is the effective solar flux at the center of the k^{th} line in units of photons/cm^2 sec Hz. According to Tousey (1964) and Tousey et al. (1964), when $\Delta\nu_D$ is appropriate to an 850° Doppler temperature the effective flux within $\Delta\nu_D$ should be given by

$$(\pi F\nu)_2 \sqrt{\pi}\, \Delta\nu_D = 5.2 \times 10^7 \text{ ph/cm}^2\text{sec}$$

$$(\pi F\nu)_1 \sqrt{\pi}\, \Delta\nu_D = 8.3 \times 10^7 \text{ ph/cm}^2\text{sec}$$

$$(\pi F\nu)_0 \sqrt{\pi}\, \Delta\nu_D = 10.4 \times 10^7 \text{ ph/cm}^2\text{sec}$$

These values assume that the solar lines are square in profile and 0.2Å wide. They are thus lower limits unless the lines are seriously reversed. In case of reversal we note that S_o would increase with decreasing altitude more rapidly than we calculate here.

In Figure (11) S_o from this solar source is plotted for the 850°K atmosphere. For the 1000° model the maximum occurs higher than for the 850°K model but has about the same maximum strength. The agreement between the predicted source shape and strength and that calculated from the airglow data would be fairly good were the solar flux about one third as great as we have taken it to be, the airglow three times as bright or there were some combination of reduced solar flux and increased airglow emission rate. The solar S_o also seems to be shifted about one scale height above the S_o required from the airglow data for the 850°K model. Increasing the oxygen content of the atmosphere does not tend to shift one curve relative to the other, but a reversal in the solar line profile could bring the solar source downward.

Furthermore, it is well to recall that the assumption of CFR is more than questionable in the last few optical depths of a very thick medium. The outgoing radiation flux is seriously reversed (Figure 2). The deficiency in the real case means that CFR, assuming as it does a flux independent of frequency overestimates the outgoing flux available for scattering near the line center. Hence it tends to underestimate the magnitude of S_o really required to produce a given scattered radiation field. This remark should serve as a caveat for attempts to deduce the density of an atmospheric constituent from the measurement of the brightness of scattered resonance radiation. Even in the optically thin boundary of an atmosphere which becomes optically thick below it is necessary to know the line profile and absolute flux of the radiation emerging from the

interior of the atmosphere as well as the external radiation to obtain the abundance of scatterers from the scattered emission rate.

The inadequency of the solar flux source in accounting for the magnitude and height profile of the 1304 airglow brightness shows clearly in Figure (11) and confirms the original conclusion of Donahue and Fastie (1964) that an internal excitation source in the F1 region is required. The profile of the source required is shown in Figure (12) for the model 8C(b). This model is chosen as the one most likely to represent realistically atmospheric conditions at the time of the Javelin experiment. Following suggestions by Dalgarno (1964) and Barth (1963) that energetic photo-electrons should provide the necessary source there have been a number of calculations of the rate of excitation of the $^3S_1$ term by this mechanism. (Tohmatsu, 1964; Green and Barth, 1967; Dalgarno et al., 1969).

In Figure (12) we show the rates calculated by Prasad (1969) and A. I. Stewart (personal communication, Dalgarno et al. 1969) for conditions similar to those assumed in our calculation. The Stewart calculation is, in fact, for the same model. The Prasad calculation is based on our 1000° model, but allows for escape of photo-electrons while Stewart assumes local energy loss. Allowance for escape should bring the Stewart curve into fairly close agreement with the required S_o above 230 km. The excitation rates have all been normalized at 170 km. That of Stewart in particular is more sharply peaked and reaches a maximum somewhat lower than the required source. However, in general the agreement between the calculated excitation rate by photo-electrons and the rate needed to explain the dayglow data is good. At low altitude absorption by O_2 requires that our values for S_o be increased below 150 km (Donahue and Strickland, 1969). The correction is about 20% at 130 km and should remove the discrepancy to be seen in Figure (12) at low altitude.

On the other hand there are other potential sources of excitation which might be significant. Two of these are dissociative processes involving O_2, one upon electron impact the other following photon absorption. The threshold for the photo-dissociative source is at 840Å and there is an edge in the absorption cross section at that wave length. The magnitude of the increase in the cross section suggests that the partial cross-section involving excitation might be about 2×10^{-17} cm^2 at 800Å (Cook and Metzger 1964).

The rate of production of the oxygen $3s\,^3S_1$ term by this process has been calculated for both the 850°K and 1000°K atmospheric models treated in this paper. Solar fluxes and absorption cross sections have been taken from the tabulations of Hinteregger et al. (1965) and the cross section for photo-dissociation estimated from the measurements of Cook and Metzger (1964). The results are Chapman layers with peak rates of 54 $cm^{-3}sec^{-1}$ at 155 km for the 1000° atmosphere and 70 $cm^{-3}sec^{-1}$ at 145 km for the 850° atmosphere. Only the flux down to 790Å is effective in this process owing to the strong absorption of N_2 below 790Å. A possible exception is the solar 304Å line which penetrates to about 120 km. A portion of this line may produce photodissociative excitation of O_2 in an important amount despite a small cross section because of the large solar flux. However, the excited atoms should have large velocities and only a small part of the radiation emitted can be imprisoned. In fact the radiation emitted from a large fraction of the excited atoms produced by dissociating O_2 may be Doppler shifted so much that it has little chance of being absorbed locally. Thus a CFR analysis of the intensity-height profile would not call for a local maximum in S_o from such a source. Although the most transparent models such as 10(a) call for a bimodal source with a maximum near the level where the dissociative process is expected to be effective, such models seem to be sufficiently

unrealistic as to lead us (regretfully) to regard this interesting feature as fortuitous.

8. Summary

Applying the techniques of radiative transfer theory to the analysis of the OI 1304Å dayglow, we have determined the initial source function or production rate of the $^3S_1$ level of oxygen starting with an observed intensity height profile and a variety of model atmospheres. The calculations have taken into account the variation of the Boltzmann temperature determining the population of the ground state levels and pure absorption by O_2. Complete frequency redistribution and a constant Doppler temperature have been assumed although different temperatures have been considered. In both the case of Doppler and the Boltzmann temperatures, non-negligible effects are observed as these are changed.

By the nature of the calculations, the solution represents excitation by all mechanisms that were actually operating during the time of the experiment. The dominant sources of excitation appear to be photoelectron impact on atomic oxygen below 400 km and resonance absorption of the 1304 solar lines above this altitude, the former being, by far, the stronger source. Additional sources of secondary importance are cascading into the ^3S level from higher states of oxygen, radiative recombination and dissociative excitation of O_2.

Appendix

To present the final workable forms of the transfer equations, we first consider the two level problem without pure absorption. Once the theory is thus formulated, we add pure absorption and finally take account of the fine structure of the oxygen ground state. Our numerical approach is to divide the medium into N variable zones, with the upper and lower boundaries of the n^{th} zone specified by the depths τ_n and τ_{n+1}. Variable zones are applied to take account of rapid variation of $S(\tau)$ near the boundaries but otherwise slow variation over the rest of the medium. At the bottom of the n^{th} zone with optical depth τ_{n+1}, the intensity has the form

$$4\pi I_n = \sum_{m=n}^{1} S_m \int_{\tau_m}^{\tau_{m+1}} T(\tau_{n+1} - \tau')d\tau' \tag{A1}$$

where S_m is the average value of $S(\tau')$ over the m^{th} zone. In terms of the so called width function

$$W_{nm} = \int_{\tau_m}^{\tau_{n+1}} T(\tau_{n+1} - \tau')d\tau' = \frac{1}{\sqrt{\pi}} \int_{-\infty}^{\infty} \left[1 - e^{-(\tau_{n+1} - \tau_m)\phi(a,x)}\right] dx \tag{A2}$$

the intensity becomes

$$4\pi I_n = \sum_{m=n}^{1} S_m (W_{nm} - W_{n,m+1}) \tag{A3}$$

$$= \sum_{m=n}^{1} S_m \Phi_{mn} \qquad m \leq n$$

The matrix Φ_{nm} is triangular and thus inversion techniques are not required to solve for S_m. Beginning with the first zone we have

$$S_1 = 4\pi I_1 / \Phi$$

followed by

$$S_2 = (4\pi I_2 - S_1 \Phi_{21}) / \Phi_{22}$$

and so on.

Once $S(\tau)$ is determined, the initial source function $S_o(\tau)$ can be found most readily if Equation (22) is written in the form (Donahue and Fastie, 1964)

$$S_o(\tau) = S(\tau)\, E\,(\tau) - \int [S(\tau') - S(\tau)]\, H(|\tau-\tau|)d\tau \qquad (A4)$$

The function $E(\tau)$, referred to as the escape function and defined by

$$E(\tau) = 1 - \int_o^{\tau_o} H(|\tau-\tau'|)d\tau' \qquad (A5)$$

is the probability that a photon originating at τ will escape the medium without being resonantly absorbed. The advantage of Equation (A4) is that S and the integral term have been modified such that their magnitudes are similar to S_o. In the form of Equation (22), an accurate solution of S_o for optical depths as large as those in this problem is not possible because of imprisonment which produces typical differences between S and S_o of three or four orders of magnitude.

In terms of N zones, Equation (A4) becomes

$$S_{on} = S_n E_n - \sum_{m=1}^{n} \int_{\tau_m}^{\tau_{m+1}} [S(\tau') - S_n]\, H(|\bar{\tau}_n-\tau'|)d\tau' \qquad (A6)$$

where the functions S_{on}, S_n, E_n, and H are referenced to $\bar{\tau}_n$, the center value of the n^{th} zone. We refer to the integral within the summation as the transport integral and designate it by

$$K_{nm} = \int_{\tau_m}^{\tau_{m+1}} [S(\tau') - S_n] \, H(|\bar{\tau}_n - \tau'|) d\tau' \qquad (A7)$$

Most of the computational work involved in obtaining an accurate solution for S_o is concerned with the proper numerical evaluation of this integral. Computationally, it is very useful to note that without pure absorption both $E(\tau)$ and $H(|\tau-\tau'|)$ are related to the function

$$\mathcal{E}(|\bar{\tau}_n - \tau'|) = \frac{1}{2\sqrt{\pi}} \int_0^1 d\mu \int_{-\infty}^{\infty} dx \; \phi(a,x) e^{-|\bar{\tau}_n - \tau'| \phi(a,x)/\mu} \qquad (A8)$$

which represents the probability that a photon emitted at τ' will travel to $\bar{\tau}_n$ without being absorbed. The relationships are

$$E(\bar{\tau}_n) = \mathcal{E}(\bar{\tau}_n) + \mathcal{E}(\tau_o - \bar{\tau}_n) \qquad (A9)$$

and

$$H(|\bar{\tau}_n - \tau'|) = \pm \frac{\partial \mathcal{E}}{\partial \tau'} \qquad (A10)$$

where $\pm$ refers to $\tau' \lesseqgtr \bar{\tau}_n$. In terms of $\mathcal{E}(|\bar{\tau}_n - \tau'|)$

$$K_{nm} = \pm \int_{\tau_m}^{\tau_{m+1}} [S(\tau') - S_n] \frac{\partial}{\partial \tau'} \mathcal{E}(|\bar{\tau}_n - \tau'|) d\tau' \qquad (A11)$$

Integration by parts leads to the following two forms of K_{nm}, the first for the case in which $S(\tau')$ is assumed not to vary within the zone and the second in which it is assumed to vary linearly as a function of τ'. For S constant

$$L_{nm} = [S_m - S_n] \, |\mathcal{E}(\Delta\tau_{n,m+1}) - \mathcal{E}(\Delta\tau_{n,m})| \qquad \text{(A12)}$$

while for a linear variation of S over each zone

$$M_{nm} = \pm \{\Delta S_{n,m+1} \, \mathcal{E}(\Delta\tau_{n,m+1}) - \Delta S_{n,m} \, \mathcal{E}(\Delta\tau_{nm}) \qquad \text{(A13)}$$

$$+ \alpha_n [\tfrac{1}{4}(W_{nm} - W_{n,m+1}) - \tfrac{1}{2}(\Delta\tau_{n,m+1} \, \mathcal{E}(\Delta\tau_{n,m+1}) - \Delta\tau_{nm} \mathcal{E}(\Delta\tau_{nm}))]\}$$

where

$$\Delta\tau_{n,m} = |\tau_n - \tau_m| \qquad \text{(A14)}$$

$$S(\tau') - S_n = \beta_n + \alpha_n |\bar{\tau}_n - \tau'|$$

and

$$\Delta S_{n,m} = S(\tau_m) - S_n$$

It is interesting to note that the term in large brackets in M_{nm} depends on the properties of the model alone and not on the source function.

Unless the zones are made so narrow and so numerous as to destroy the advantages for which the technique of zone division is designated, the approximation that S is constant for each zone can lead to serious error. Because H' decreases as τ' varies across the zone, the effective average value of $S(\tau')$ is found closer to τ_n than the center of the zone. The error arises in the transport integral because S_n is subtracted from $S(\tau')$ and the difference becomes very sensitive to $S(\tau')$ when $S(\tau') \approx S_n$. Approximating

the real $S(\tau')$ by a linear function over each zone considerably improves the accuracy of K_{nm} and this approximation has been used to obtain the results in this paper. In terms of M_{nm} the transport equation for S_o may now be written as

$$S_{on} = S_n E_n + \sum_{m=1}^{n} M_{nm} \tag{A15}$$

a form expressed in terms of the transport functions $W(\tau)$ and $\mathcal{E}(\tau)$.

Two effects complicate these procedures for obtaining $S(\tau)$ and $S_o(\tau)$ in the aurora and airglow. One is absorption of the resonance photons by molecular oxygen, the other is the triplet nature of the radiation. Keeping to the two level formulation of the theory for the present, absorption by O_2 can be taken into account when $S(\tau)$ is deduced from $4\pi I(\tau)$ by letting a_{nm} be the optical depth for absorption by O_2 between the center of the m^{th} zone and τ_{n+1}. The transmission function in Equation (A1) then becomes $T'(\tau_{n+1} - \tau', t_{n+1} - t')$ as defined in Equation (26). The result is that Equation (A3) is then changed to

$$4\pi I_n = \sum_{m=n}^{I} S_m e^{-a_{nm}} (W_{n,m} - W_{n,m+1}) \tag{A16}$$

The effect is to increase the values of S_m in regions where absorption is appreciable.

Similarly, in the transport Equations (A4) and (A6) $H'(|\tau - \tau'|, |t - t'|)$ as given by Equation (27) must replace $H(|\tau - \tau'|)$. The transport integral (A7) becomes

$$K_{nm} = \int_{\tau}^{\tau_{m+1}} [S(\tau') - S_n] \, H'(|\bar{\tau}_n - \tau'|, |\bar{t}_n - t'|) \, d\tau' \tag{A17}$$

If t' is taken to be constant through each zone then

$$H'(|\tau_n - \tau'|, |\bar{t}_n - t'|) = \pm \frac{\partial}{\partial \tau'} \; {}_1(|\tau_n - \tau'|, |\bar{t}_n - t'|); \quad \begin{matrix} \tau' < \bar{\tau}_n \\ \tau' > \bar{\tau}_n \end{matrix} \tag{A18}$$

where

$${}_1(|\tau_n - \tau', t_{nm}) = \frac{1}{2\sqrt{\pi}} \int_0^1 d\mu \int_{\infty}^{\infty} dx \; \phi(a,x) \; e^{-(|\bar{\tau}_n - \tau'|\phi(a,x) + t_{nm})/\mu} \tag{A19}$$

$$= \frac{1}{2\sqrt{\pi}} \int_{\infty}^{\infty} \phi(a,x) \; E_2[(|\bar{\tau}_n - \tau'| \; \phi(a,x) + t_{nm})] \; dx$$

Here t_{nm} is the optical depth in O_2 from the center of strip n to the center of strip m and E_2 is the second exponential integral.

If, however, we consider a linear variation in the t' across a zone expressed by

$$|\bar{t}_n - t'| = \alpha_t |\tau_n - \tau'| + \beta_t \tag{A20}$$

H' is defined as the divergence of $\mathcal{E}_2$ where

$$\mathcal{E}_2(|\bar{\tau}_n - \tau'|, \; |\bar{t}_n - t'|, \; \alpha_t)$$

$$= \frac{1}{2\sqrt{\pi}} \int_{-\infty}^{\infty} \frac{\phi^2(a,x)}{\phi(a,x) + \alpha_t} E_2(|\bar{\tau}_n - \tau'|\phi(a,x) + |\bar{t}_n - t'|)dx \tag{A21}$$

For $m \neq n$, the effect on K_{nm} of replacing t_{nm} by a variable absorption for each zero is very small. Therefore, in practice, O_2 absorption between zone n and m is taken into account by using the function $\mathcal{E}_1$ in evaluating the kernel H'. We need not even consider the case m = n since by the nature of

K_{nm}, this term is virtually zero. Now L_{nm}, the transport integral which applies to the case of constant $S(\tau')$ in each zone, may be written in the form

$$L_{nm} = [S_m - S_n] \left| \mathcal{E}_1(\Delta\tau_{n,m+1}, t_{nm}) - \mathcal{E}_1(\Delta\tau_{nm}, t_{nm}) \right| \tag{A22}$$

The second form M_{nm}, appropriate in the case of a linear variation in $S(\tau')$ over each zone, becomes

$$M_{nm} = \pm \left\{ [S(\tau') - S_n] \mathcal{E}_1(|\bar{\tau}_n - \tau'|, t_{nm}) \Big|_{\tau}^{\tau_{m+1}} \right. \\ \left. \pm \alpha_n \int_{\tau_n}^{\tau_{m+1}} \mathcal{E}_1(|\bar{\tau}_n - \tau'|, t_{nm}) d\tau' \right\} \tag{A23}$$

after an integration of Equation (A17) by parts. After some manipulation, the integral term takes the form

$$\int \mathcal{E}_1 \, d\tau' = \pm \left\{ \frac{e^{-t_{nm}}}{4} (W_{n,m} - W_{n,m+1}) \right. \\ - \frac{1}{2}[\Delta\tau_{n,m+1} \mathcal{E}_1(\Delta\tau_{n,m+1}, t_{nm}) - \Delta\tau_{n,m} \mathcal{E}_1(\Delta\tau_{nm}, t_{nm})] \\ \left. - \mathcal{E}_{nm}(t_{nm}) \right\} \tag{A24}$$

where

$$\mathcal{E}_{nm}(t_{nm}) = \frac{1}{4\pi} t_{nm} \int_{-\infty}^{\infty} \left[E_2(\Delta\tau_{n,m+1} \phi(a,x) + t_{nm}) - E_2(\Delta\tau_{n,m} \phi(a,x) + t_{nm}) \right] dx$$

Insertion of Equation (A24) in Equation (A23) leads to the final two level form for M_{nm}

$$M_{nm} = \pm \{\Delta S_{n,m+1} \mathcal{E}_1(\Delta\tau_{n,m+1}, t_{nm}) - \Delta S_{n,m} \mathcal{E}_1(\Delta\tau_{n,m}, t_{nm})$$

$$+ \alpha_n [\frac{e^{-t_{nm}}}{4} (W_{n,m} - W_{n,m+1}) - \frac{1}{2} (\Delta\tau_{n,m+1} \mathcal{E}_1(\Delta\tau_{n,m+1}, t_{nm}) \quad \text{(A26)}$$

$$- \Delta\tau_{n,m} \mathcal{E}_1(\Delta\tau_{n,m}, t_{nm})) - \epsilon_{nm}(t_{nm})]$$

which is to replace the earlier version in Equation (A13).

The escape function E_n must also be modified to accommodate pure absorption. Beginning with the definition of Equation (A5) and using Equation (A10) this function becomes

$$E_n = 1 - \sum_{m=1}^{n} \int_{\tau_m}^{\tau_{m+1}} (\pm) \frac{\partial}{\partial\tau'} \mathcal{E}(|\tau_n - \tau'|, |t_n - t'|)\, d\tau' \quad \text{(A27)}$$

The sum is often very close to unity and E_n very small for an optically thick medium. The largest contribution to the series, even if $\Delta\tau_n$ is of the order of say 50 comes from the n^{th} strip itself since most absorption occurs very close to the point of origin to the photons. Near the origin, it is desirable to approximate pure absorption by a linear function rather than by an average value. Hence, for the n^{th} zone itself, we have used the transport function $\mathcal{E}_2$ in the integrand. In contrast to the dominance of the n^{th} term in E_n, we were able to ignore M_{nn} and hence the function $\mathcal{E}_2$ as well in the evaluation of the transport integral.

Evaluation of the integral in Equation (A27) with n = m yields the value

$$2[\mathcal{E}_2(0,0,\alpha_t{}^n) - \mathcal{E}_2(\frac{\Delta\tau_n}{2}, \frac{\Delta t_n}{2}, \alpha_t{}^n)] \quad \text{(A28)}$$

For the other zones it is sufficient to consider t' constant in each zone and use the form $\mathcal{E}_1$ in the integrands. This leads to

$$\int_{\tau_m}^{\tau_{m+1}} \frac{\partial}{\partial \tau'} \mathcal{E}_1 \, d\tau' = \mathcal{E}_1(\Delta\tau_{n,m+1}, t_{nm}) - \mathcal{E}_1(\Delta\tau_{nm}, t_{nm}) \qquad \text{(A29)}$$

Thus

$$E_n = 1 - 2[\mathcal{E}_2(0,0,\alpha_t^n) - \mathcal{E}_2(\frac{\Delta\tau_n}{2}\frac{\Delta t_n}{2},\alpha_t^n) + \sum_{m \neq n} |\mathcal{E}_1(\Delta\tau_{n,m+1}, t_{nm}) - \mathcal{E}_1(\Delta\tau_{n,m}, t_{nm})| \qquad \text{(A30)}$$

It is interesting to note that the addition of pure absorption actually increases the "escape" probability since by definition, escape here refers to loss from the medium without a resonance absorption.

Finally the extension of this treatment to the three lines at 1302, 1304 and 1306Å is simple. The intensity becomes

$$4\pi I_n = \sum_{m=n}^{1} S_m(\tau_2) \sum_j g'_j \left(\frac{p_2}{P_J}\right)_m e^{-a_{nm}} \left(W_j^{nm} - W_j^{n,m+1}\right) \qquad \text{(A31)}$$

while the transport solution becomes

$$S_{on}(\tau_2) = S_n(\tau_2) E_n + \sum_{m=1}^{n} \sum_k g'_k \left(\frac{p_k}{p_2}\right)_n M_k^{nm} \qquad \text{(A32)}$$

where S_o and S are expressed in terms of depth τ_2. The escape function in Equation (A32) is now the sum of probabilities of escape in each of the three lines, i.e.,

$$E_n = 1 - \sum_j \{g_j' \, 2[\mathcal{E}_2(0,0,\alpha_t^{n_j}) - \mathcal{E}_2(\frac{\Delta\tau_j^n}{2},\frac{\Delta t^n}{2},\alpha_t^{n_j})] + \sum_{m \neq n} g_j' \, |\mathcal{E}_1(\Delta\tau_j^{n,m+1}, t^{nm}) - \mathcal{E}_1(\Delta\tau_j^{n,m}, t^{nm})|\} \qquad \text{(A33)}$$

In summary we have reduced the transport integral and the escape function to expressions involving the transport functions W_{nm} (Equation (A2)), $\mathcal{E}$ (Equation (A8)), $\mathcal{E}_1$ (Equation (A19)) and $\mathcal{E}_2$ (Equation (A21)). We considered four cases for the transport integral:

1) No pure absorption
   a) $S(\tau)$ constant over a given zone; Equation (A12)
   b) $S(\tau)$ linear over a given zone; Equation (A13)
2) Pure absorption included
   a) $S(\tau)$ constant; Equation (A22)
   b) $S(\tau)$ linear; Equation (A26)

Corresponding to the transport integral are two cases for the escape function:

1) No pure absorption; Equation (A9)
2) Pure absorption included: Equation (A30).

Acknowledgements

The research reported in this paper was supported in part by the National Aeronautics and Space Administration (Contract NASr 179), and the National Science Foundation, Atmospheric Sciences Division (Aeronomy) GA-1237.

References

Barth, C. A., Communication to Aeronomy Symposium IUGG, Berkeley, Calif., 1963.

Colegrove, F. D., F. S. Johnson, and W. B. Hanson, J. Geophys. Res. 71, 2227, 1966.

Cook, G. R. and P. H. Metzger, J. Chem. Phys. 41, 321, 1964.

Dalgarno, A., Ann. Geophys. 20, 67, 1964.

Dalgarno, A. and T. C. Deggis, Planet. Space Sci. 16,125, 1968.

Dalgarno, A., M. B. McElroy, and A. I. Stewart, J. Atmosph. Sci., 1968 (in press).

Donahue, T. M. and W. G. Fastie, Space Res. IV, 304, 1964.

Donahue, T. M., Planet. Space Sci. 13, 871, 1965.

Donahue, T. M. and D. J. Strickland, Planet. Space Sci., 1969 (to be submitted).

Doschek, G. A., Astrophys. J., to be published, 1969.

Fastie, W. G., H. M. Crosswhite, and D. F. Heath, J. Geophys. Res. 69, 4129, 1964a.

Fastie, W. G. and H. M. Crosswhite, Planet. Space Sci. 12, 1026, 1964b.

Fastie, W. G., Planet. Space Sci. 16, 929, 1968.

Garstang, R. H., Proc. Phil. Soc. (Cambridge) 57, 115, 1961.

Green, A. E. S. and C. A. Barth, J. Geophys. Res. 72, 3975, 1967.

Hearn, A. G., Proc. Phys. Soc. 84, 11, 1968.

Heath, D. F., Goddard Space Flight Center, Report X-662-68-31, 1968.

Henyey, L. G., Proc. Nat. Acad. Sci. 26, 50, 1940.

Holstein, T., Phys. Rev. 72, 1212, 1947.

Hummer, D. G., Mon. Not. R. Astr. Soc. 125, 21, 1962.

Jacchia, L. G., Space Res. V, 1152, 1965.

Kaplan, S. A., V. V. Katyushina, and V. G. Kurt, 5th Int'l. Space Science Symposium and Cospar Meeting, Florence, Italy, 1964.

Kelly, P. S., Astrophys. J. 140, 1247, 1964.

Lawrence, G. M., Can. J. Chem. 47, 1856, 1969.

Lee, P., J. Opt. Soc. Am. 45, 703, 1955.

Mitchell, A. C. G., and M. W. Zemansky, Cambridge University Press, New York, 1961.

Parkes, D. A., L. F. Keyser, and F. Kaufman, Astrophys. J. 149, 217, 1967.

Prag, A. B., C. E. Fairchild, and K. C. Clark, Phys. Rev. 137, A1328, 1965.

Prasad, S. S., J. Ge phys. Res. 1969 (in press).

Tohmatsu, T., Rep. Ionosph. Space Res. (Japan) 18, 425, 1964.

Tohmatsu, T., Rep. Ionosph. Space Res. (Japan) 19, 509, 1965.

Tousey, R., Space Sci. Rev. 2, 3, 1964a.

Tousey, R., J. D. Purcell, W. E. Austin, D. L. Garrett, and K. G. Widing, Space Res. IV, 703, 1964b.

U. S. Standard Atmosphere Supplement, U.S. Government Printing Office, Washington, D. C., 1966.

FIGURE CAPTIONS

1. Directional and frequency dependent CFR intensity profiles. Because of considerably greater optical depths along the line of sight in the downward direction ($\theta = 180°$) the corresponding profiles at large x are greater than those for the upward observing direction.
2. Directional and frequency dependent CFR intensity profiles near the upper boundary.
3. Smoothed experimental 1304 intensity height profile including the low altitude data of Fastie et al. (1964) and high altitude data of Fastie (1968).
4. Behavior of $S(\tau_2)$ near the upper boundary for models with exospheric temperatures of 850° and 1000°. The dashed curves represent $S(\tau_2)$ for the case which ignores attenuation from the point of emission to the point of observation.
5. Total source functions S(z) for the 850° exospheric temperature model. The solutions show the effect of changing T_B. In each case $T_D = 300°$.
6. Initial source functions $S_0(z)$ corresponding to the S(z)'s of Fig. 5.
7. Total source functions S(z) for the 850° exospheric temperature model. The solutions show the effect of changing T_D from 300° in model 3C to 850° in model 8C. In each case, $T_B = 1000°$.
8. Initial source functions $S_o(z)$ corresponding to the S(z)'s of Fig. 7.
9. Initial source functions $S_o(z)$ of Fig. (6) and (8) shown for comparison. Included on the abscissa is the temperature profile of the 850° exospheric temperature model.
10. Initial source functions for the 1000° exospheric temperature model and f = .021 shown for comparison among themselves and to compare with those of Fig. 9 which pertain to f = .046.

11. The initial source functions $S_o^{8C(b)}(z)$ and $S_o^{10(c)}(z)$ for the 850^o and 1000^o exospheric temperature models extended to high altitudes and the solar resonance production rate determined explicitly by Equation (39).
12. Initial source function $S_o^{8C}(z)$ and production rates determined for photoelectron impact excitation on OI. All solutions refer to a solar zenith angle of 60^o. The 850^o model was used to determine $S_o(z)$ as well as Stewart's solution while the 1000^o model was used to determine Prasad's solution.

Table 2. Boltzmann factors for the triplet levels of the ground state of OI.

T	P_2	P_1	P_0
200	.812	.156	.032
500	.674	.256	.070
1000	.617	.294	.089
∞	.555	.333	.111

Table 3. 850° Exospheric Temperature Model

z(Km)	T(°K)	n(0)	$n(0_2)$	τ_2	τ_1	τ_0
100	208	5.00(11)	1.99(12)	7.19(4)	1.92(4)	4.63(3)
120	355	7.60(10)	7.50(10)	1.58(4)	6.20(3)	1.73(3)
150	643	1.43(10)	4.83(9)	5.25(3)	2.32(3)	6.79(2)
200	801	3.42(9)	3.44(8)	1.57(3)	7.17(2)	2.13(2)
250	838	1.12(9)	3.87(7)	5.47(2)	2.51(2)	7.44(1)
300	847	3.97(8)	4.90(6)	2.00(2)	9.17(1)	2.72(1)
350	849	1.45(8)	6.52(5)	7.41(1)	3.40(1)	1.01(1)
400	850	5.37(7)	8.99(4)	2.78(1)	1.28(1)	3.80(0)
450	850	2.05(7)	1.15(4)	1.07(1)	4.90(0)	1.46(0)
500	850	7.74(6)	1.87(3)	4.12(0)	1.89(0)	5.61(-1)
600	850	1.18(6)	4.33(1)	6.24(-1)	2.87(-1)	8.50(-2)
700	850	1.76(5)	1.00(0)	9.77(-2)	4.48(-2)	1.33(-2)

Table 4. 1000° Exospheric Temperature Model

z(Km)	(T°K)	n(o)	$n(O_2)$	τ_2	τ_1	τ_0
100	220	2.83(11)	2.90(12)	3.26(4)	1.04(4)	2.58(3)
120	347	9.65(10)	1.14(11)	1.04(4)	4.08(3)	1.14(3)
150	661	1.64(10)	6.52(9)	3.35(3)	1.52(3)	4.50(2)
200	893	3.93(9)	5.04(8)	1.08(3)	5.12(2)	1.54(2)
250	990	1.41(9)	7.10(7)	4.32(2)	2.06(2)	6.24(1)
300	1000	5.80(8)	1.22(7)	1.83(2)	8.74(1)	2.64(1)
350	1000	2.46(8)	2.19(6)	7.89(1)	3.77(1)	1.14(1)
400	1000	1.05(8)	4.07(5)	3.45(1)	1.65(1)	4.98(0)
500	1000	2.03(7)	1.52(4)	6.84(0)	3.27(0)	9.87(-1)
600	1000	4.13(6)	6.20(2)	1.42(0)	6.79(-1)	2.05(-1)
700	1000	8.72(5)	2.78(1)	3.04(-1)	1.45(-1)	4.39(-2)

Table 5. Models used to obtain transport solutions for the f values .021 and .046

f = .021			f = .046					
T_{ex} = 1000°			T_{ex} = 850°			T_{ex} = 1000°		
Model number	T_D(°K)	T_B(°K)	Model number	T_D(°K)	T_B(°K)	Model number	T_D(°K)	T_B(°K)
3V(a)	300	variable	3V(b)	300	variable	10C(c)	1000	1000
3C(a)	300	1000	3C(b)	300	1000			
10V(a)	1000	variable	8V(b)	850	variable			
10C(a)	1000	1000	8C(b)	850	1000°			

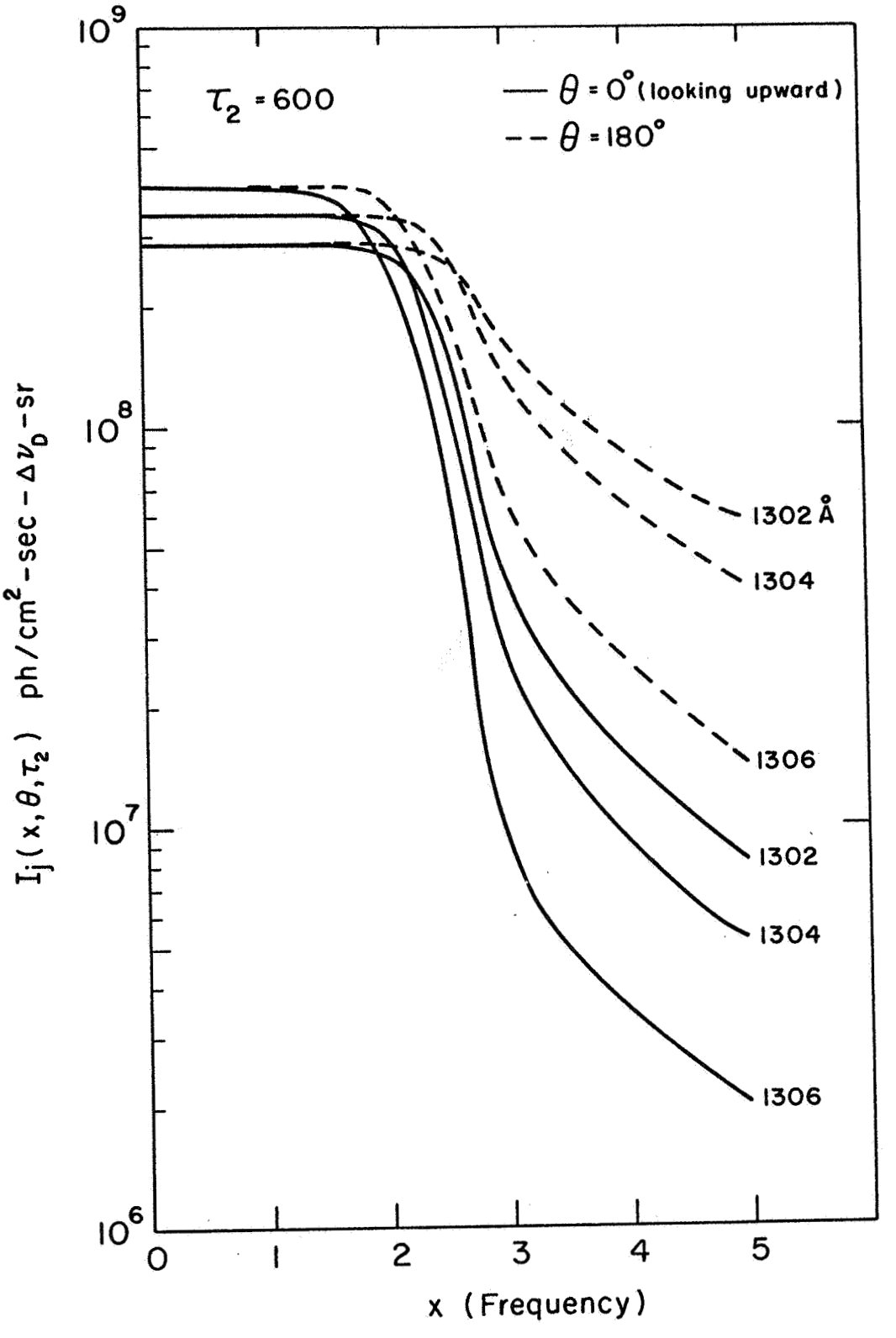
10^9
10^8
10^7
10^6
$\tau_2 = 600$
$\theta = 0°$ (looking upward)
$\theta = 180°$
1302 Å
1304
1306
1302
1304
1306
0
1
2
3
4
5
x (Frequency)
$I_j(x, \theta, \tau_2)$ ph/cm^2-sec-$\Delta\nu_D$-sr

Figure 1

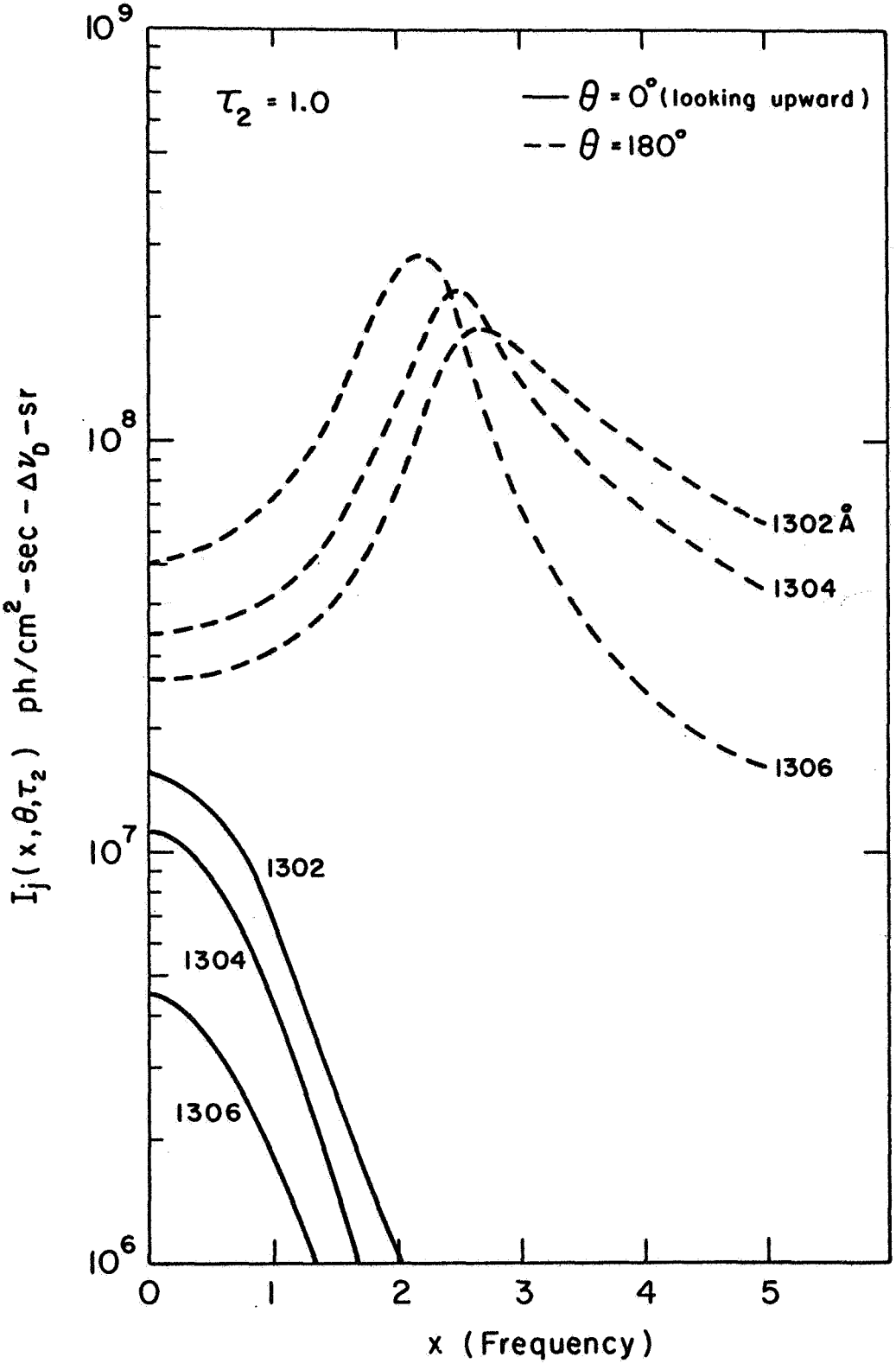
10^9
10^8
10^7
10^6
τ_2 = 1.0
— θ = 0° (looking upward)
-- θ = 180°
1302 Å
1304
1306
1302
1304
1306
$I_j(x, \theta, \tau_2)$ ph/cm^2-sec-$\Delta\nu_0$-sr
0
1
2
3
4
5
x (Frequency)

Figure 2

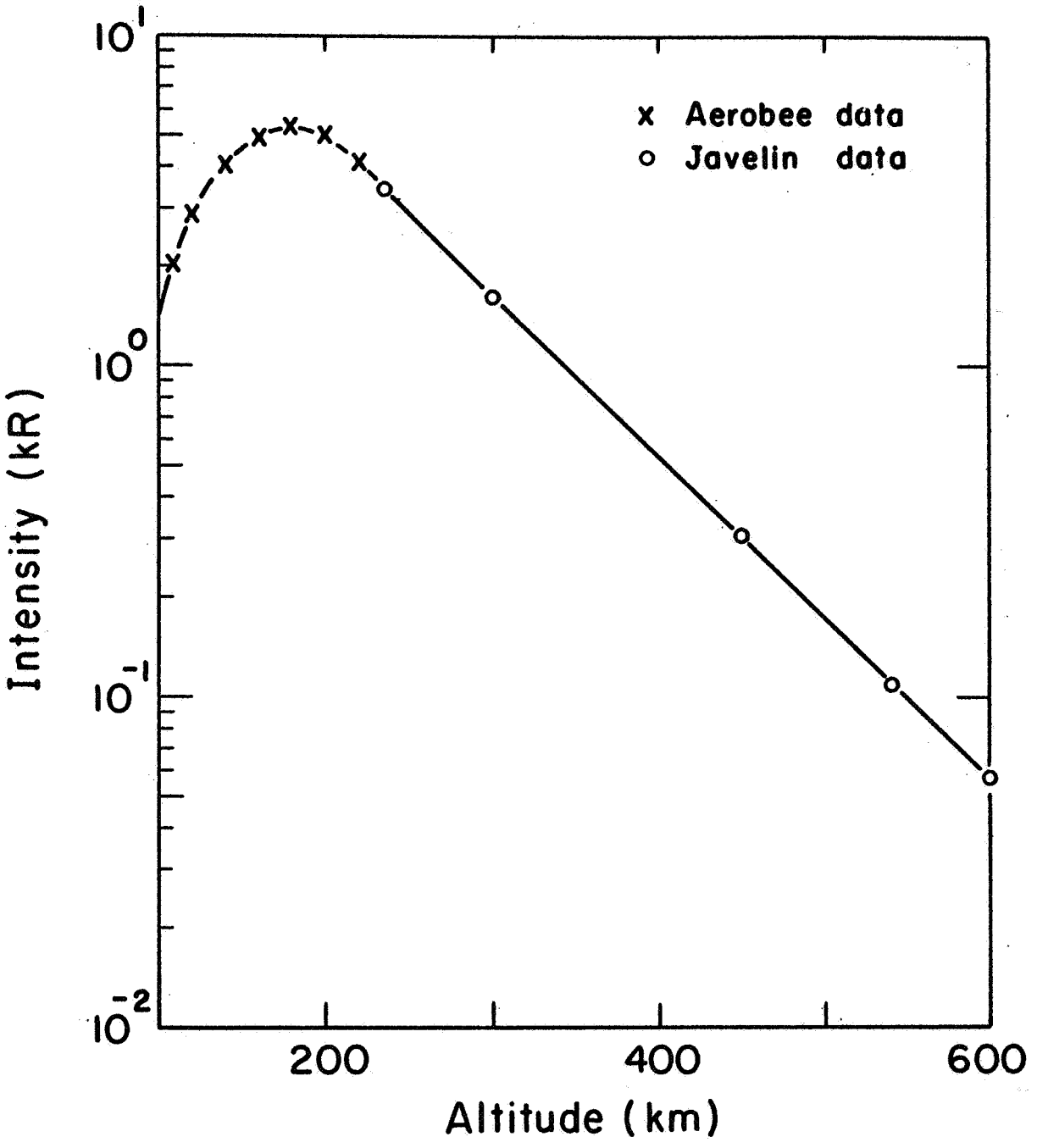
x Aerobee data
o Javelin data
Intensity (kR)
10^1
10^0
10^-1
10^-2
200
400
600
Altitude (km)

Figure 3

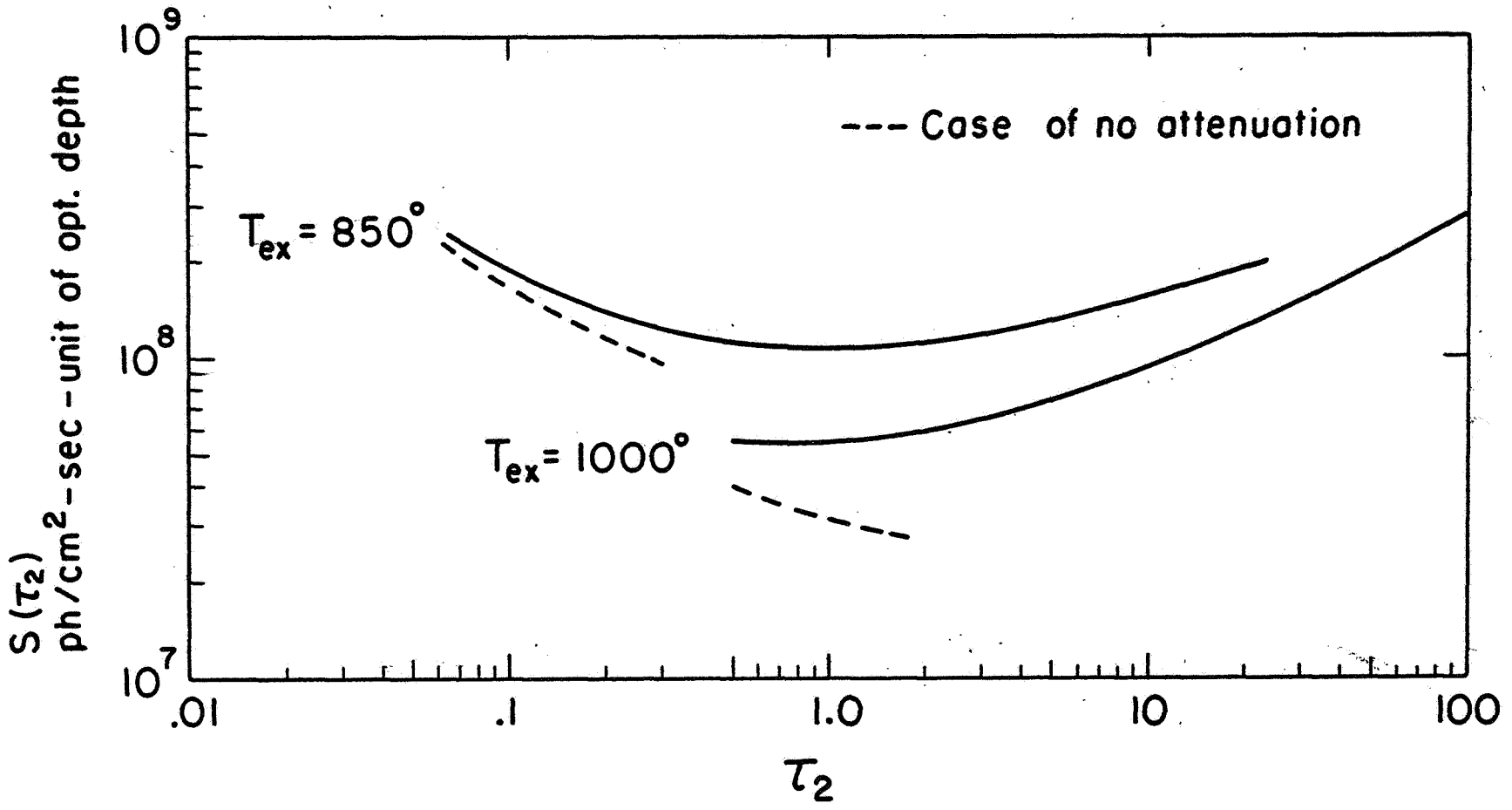
10^9
10^8
10^7
$S(\tau_2)$ ph/cm^2-sec-unit of opt. depth
--- Case of no attenuation
T_{ex} = 850°
T_{ex} = 1000°
.01
.1
1.0
10
100
τ_2

Figure 4

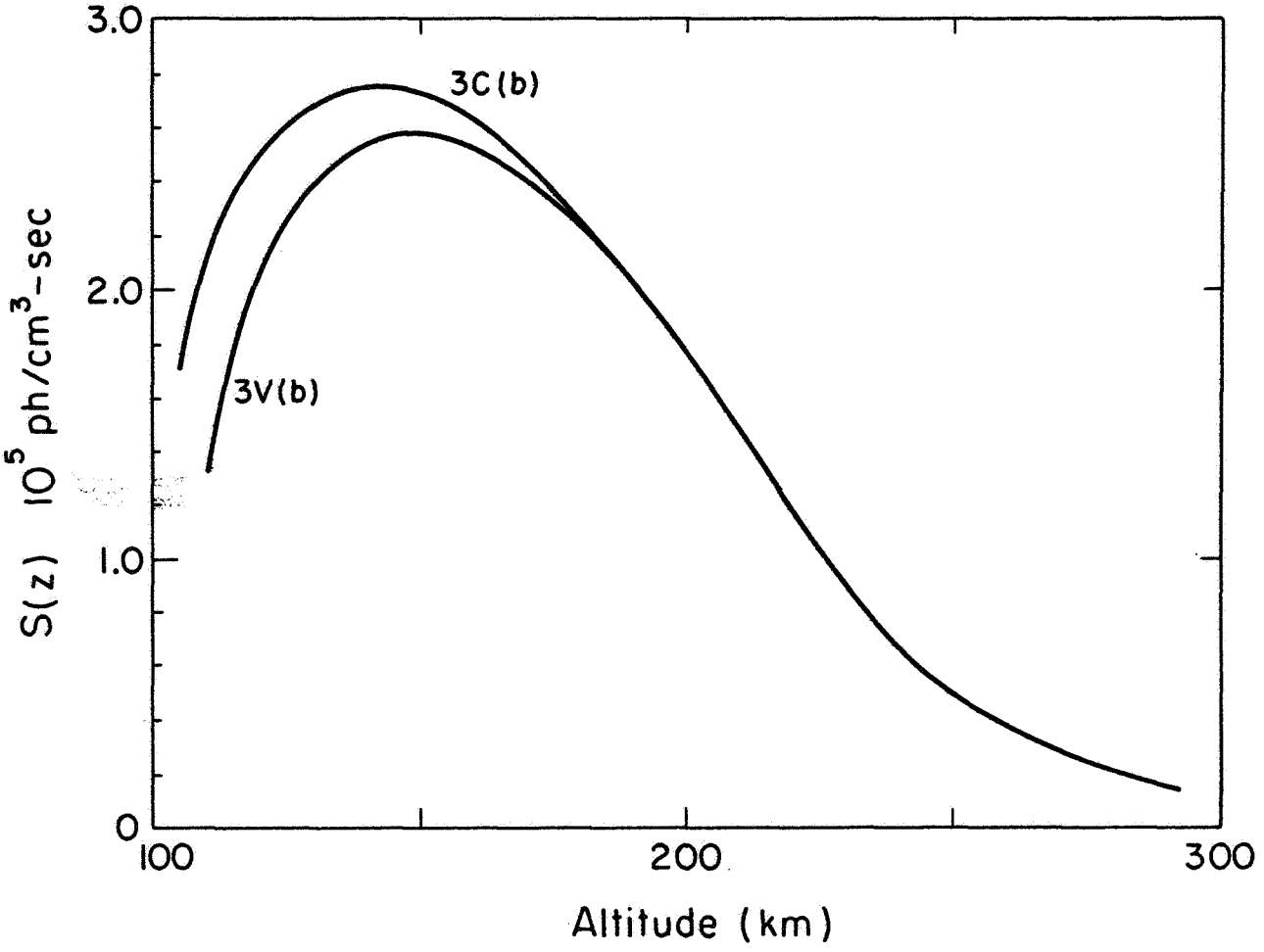

Figure 5

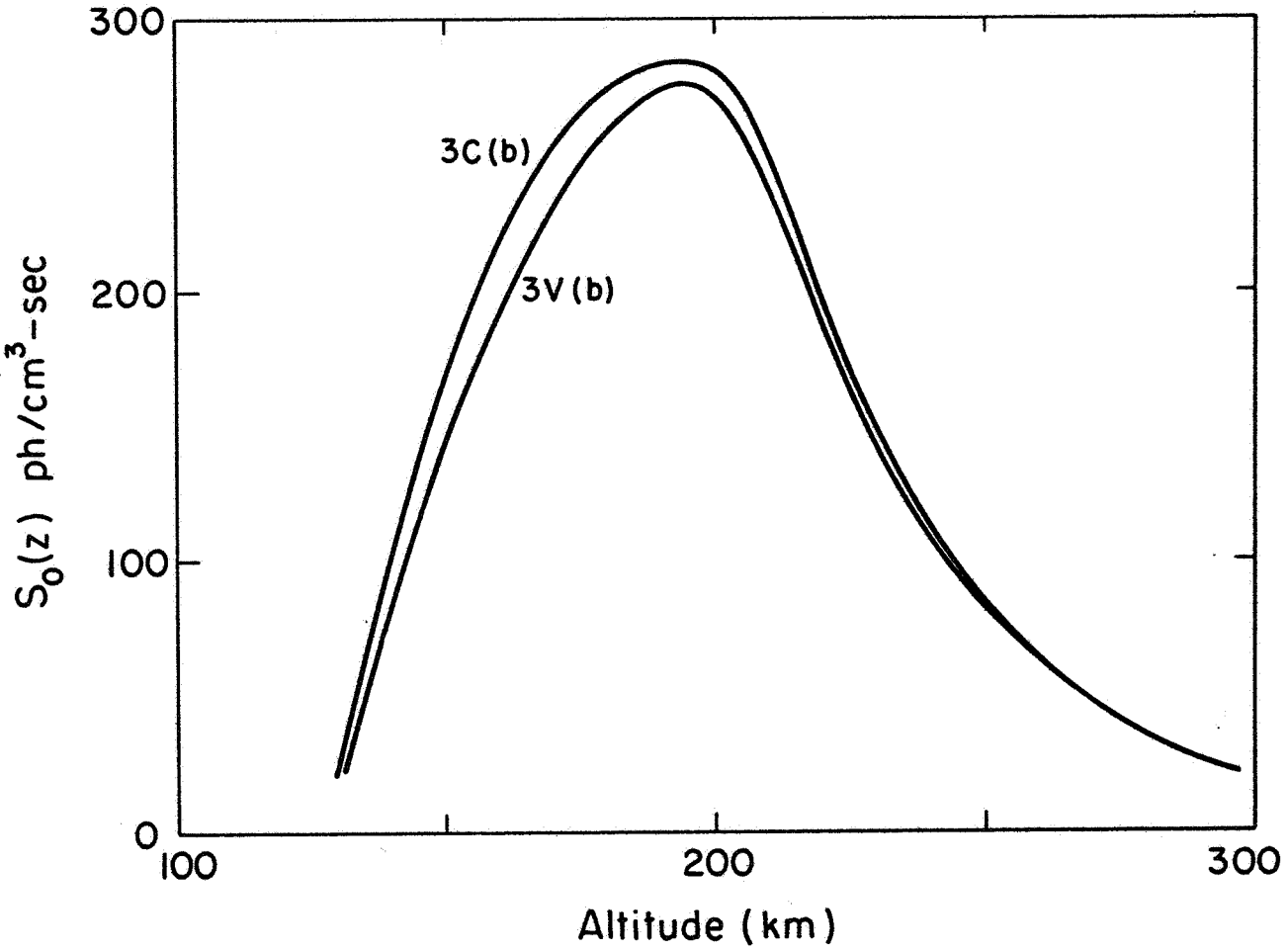

Figure 6

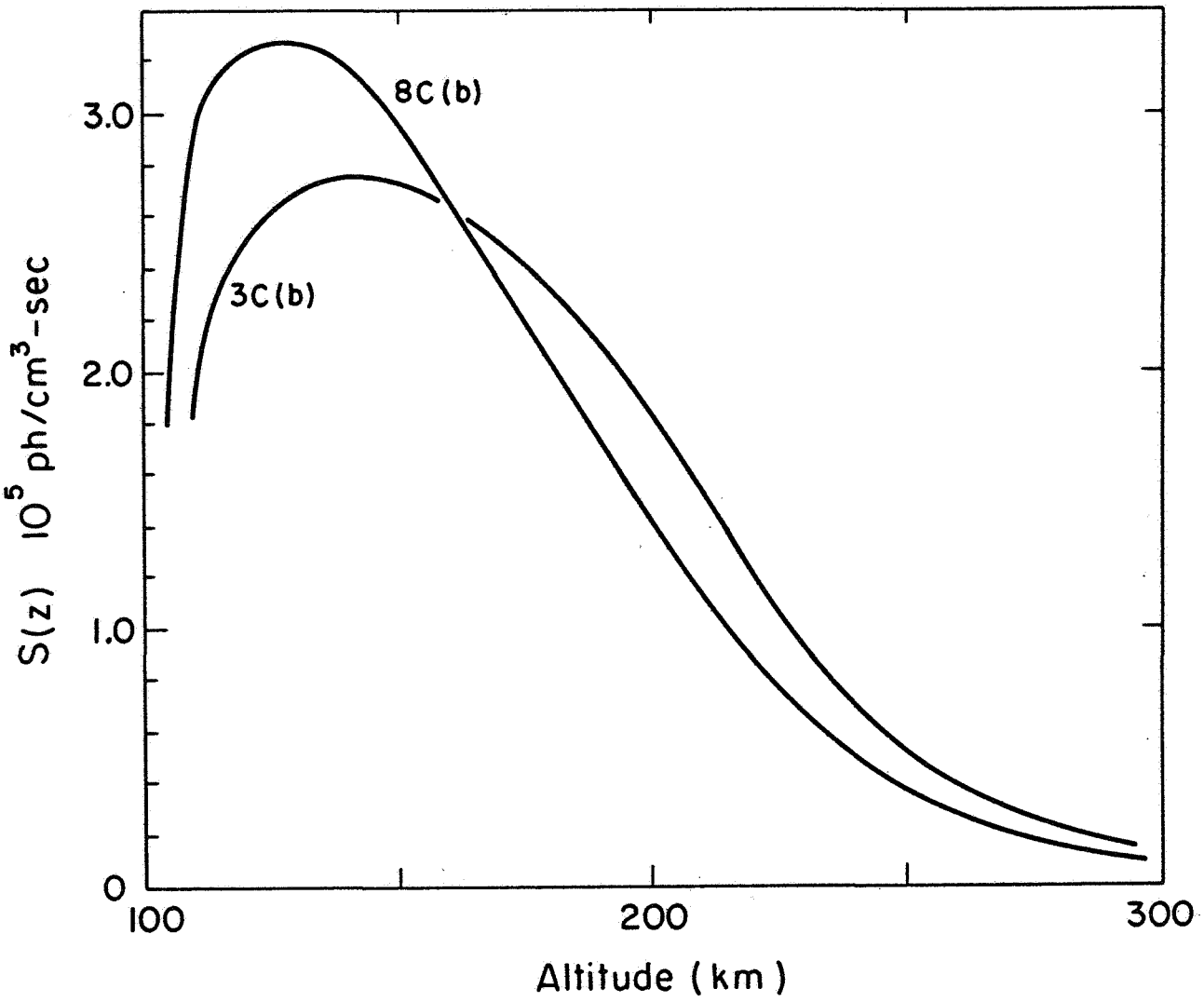

Figure 7

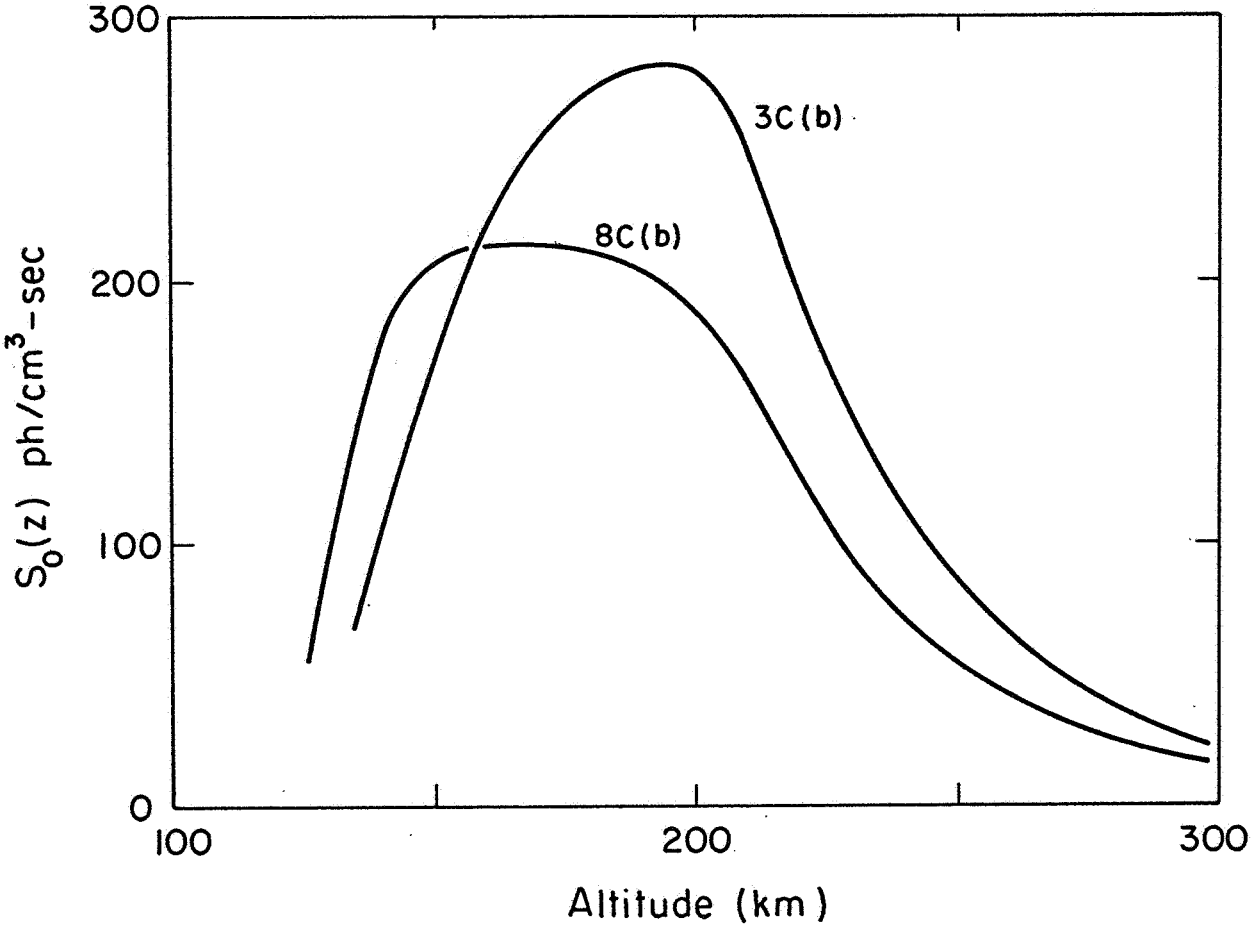

Figure 8

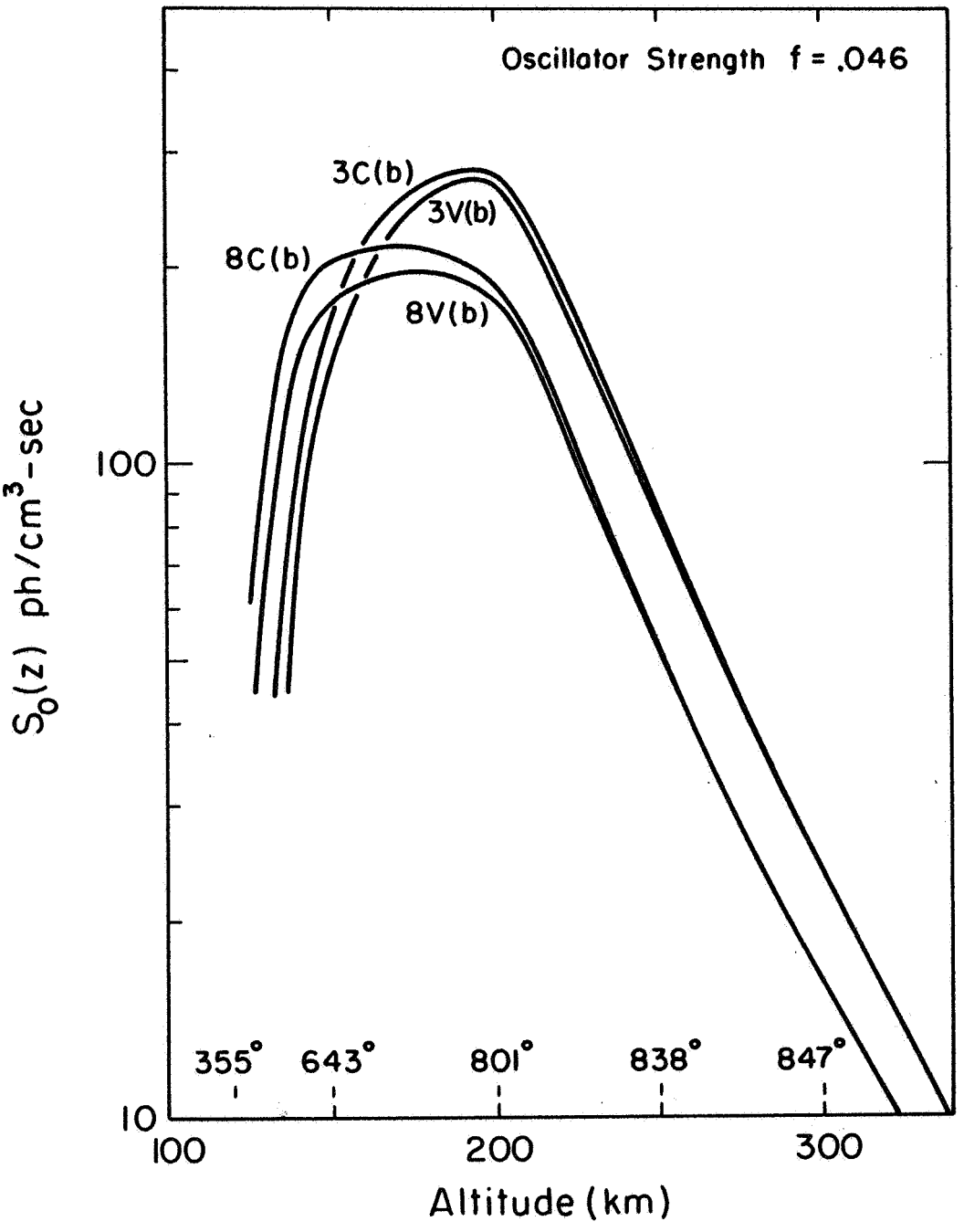
Oscillator Strength f = .046
3C(b)
3V(b)
8C(b)
8V(b)
100
10
$S_0(z)$ ph/cm^3-sec
355°
643°
801°
838°
847°
100
200
300
Altitude (km)

Figure 9

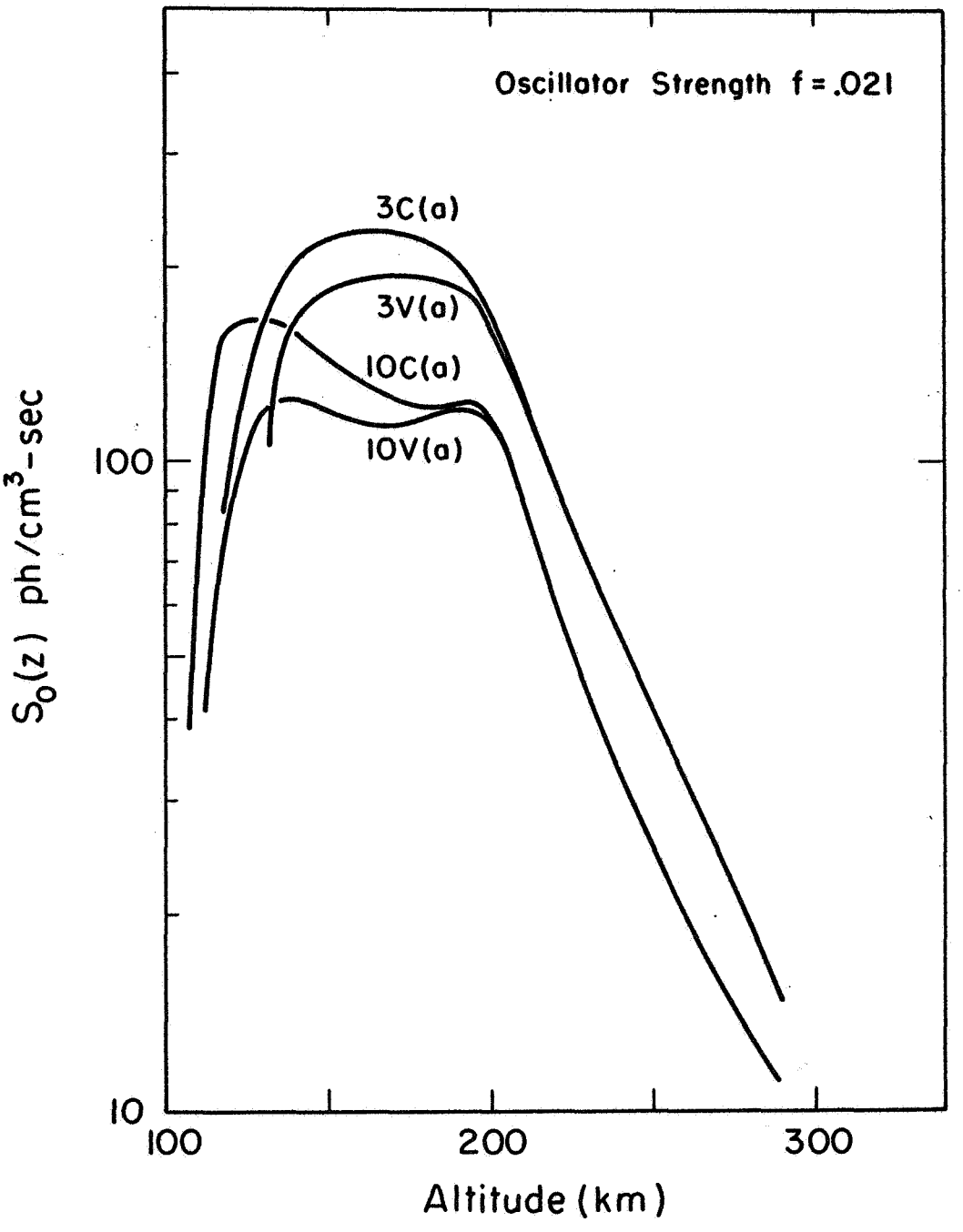
Oscillator Strength f = .021
3C(a)
3V(a)
10C(a)
10V(a)
100
10
100
200
300
Altitude (km)
$S_0(z)$ ph/cm^3-sec

Figure 10

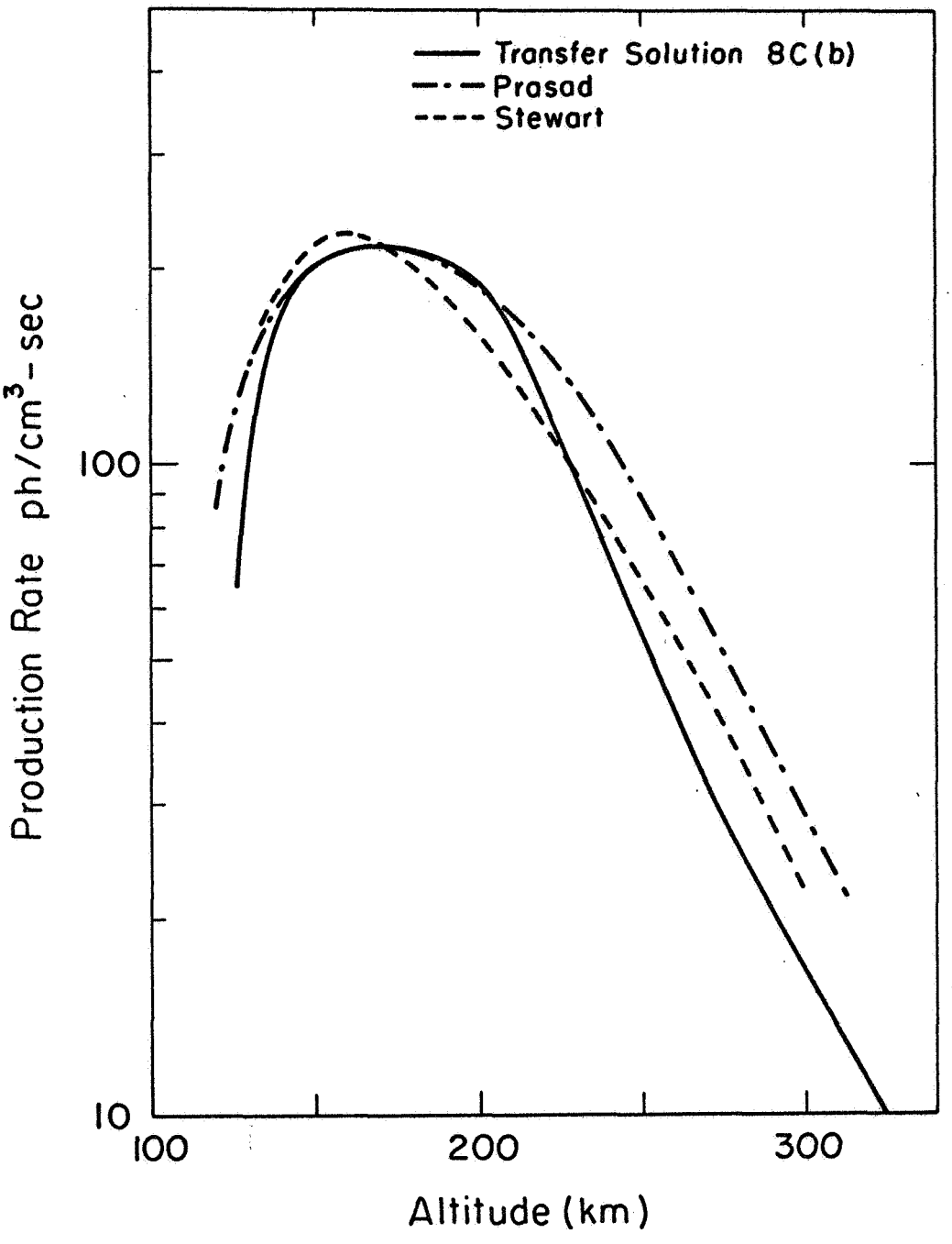
Transfer Solution 8C(b)
Prasad
Stewart
Production Rate ph/cm³-sec
100
10
100
200
300
Altitude (km)

Figure 11

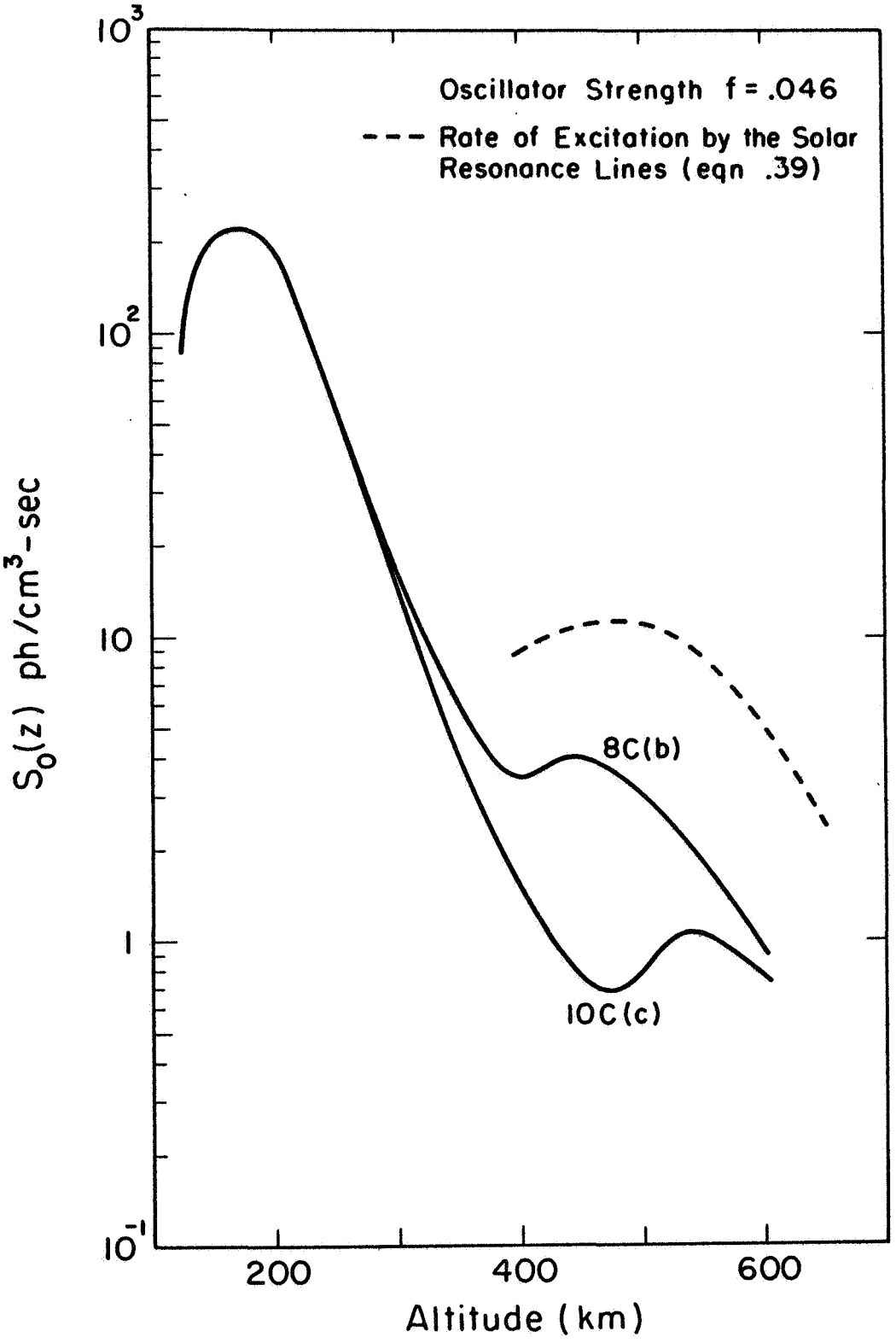
Oscillator Strength f = .046
--- Rate of Excitation by the Solar Resonance Lines (eqn .39)
8C(b)
10C(c)
10^3
10^2
10
1
10^{-1}
$S_0(z)$ ph/cm^3-sec
200
400
600
Altitude (km)

Figure 12